

Signals of vagal circuits engaging with AKT1 in $\alpha 7$ nAChR⁺CD11b⁺ cells lessen *E. coli* and LPS-induced acute inflammatory injury

Caiqi Zhao¹, Xi Yang¹, Emily M Su², Yuanyuan Huang¹, Ling Li¹, Michael A Matthay^{3,*}, Xiao Su^{1,*}

¹CAS Key Laboratory of Molecular Virology & Immunology, Unit of Respiratory Infection and Immunity, Institut Pasteur of Shanghai, Chinese Academy of Sciences, University of Chinese Academy of Sciences, Shanghai, China; ²Dana Farber Cancer Institute, Boston, MA, USA; ³Cardiovascular Research Institute, University of California, San Francisco, CA, USA

Vagal circuits- $\alpha 7$ nAChR ($\alpha 7$ nicotinic acetylcholine receptor, coded by *Chrna7*) signaling utilizes spleen as a hub to dampen systemic inflammatory responses. Vagal innervations also extend to the distal airways and alveoli. Vagotomy and deficiency of $\alpha 7$ nAChR deteriorate *E. coli* and lipopolysaccharide (LPS)-induced acute lung inflammatory responses; however, the underlying mechanisms remain elusive. Here, we hypothesized that vagal circuits would limit splenic release and lung recruitment of $\alpha 7$ nAChR⁺CD11b⁺ cells (CD11b is coded by *Itgam*, a surface marker of monocytes and neutrophils) via phosphorylation of AKT1 and that this process would define the severity of lung injury. Using both *E. coli* and LPS-induced lung injury mouse models, we found that vagotomy augmented splenic egress and lung recruitment of $\alpha 7$ nAChR⁺CD11b⁺ cells, and consequently worsened lung inflammatory responses. Rescue of vagotomy with an $\alpha 7$ nAChR agonist preserved $\alpha 7$ nAChR⁺CD11b⁺ cells in the spleen, suppressed recruitment of these cells to the lung and attenuated lung inflammatory responses. Vagal signals via $\alpha 7$ nAChR promoted serine473 phosphorylation of AKT1 in $\alpha 7$ nAChR⁺CD11b⁺ cells and stabilized these cells in the spleen. Deletion of *Akt1* enhanced splenic egress and lung recruitment of $\alpha 7$ nAChR⁺CD11b⁺ cells, which elicited neutrophil-infiltrated lung inflammation and injury. Vagotomy and double deletion of *Chrna7* and *Itgam* reduced serine473 phosphorylation of AKT1 in the spleen and BAL (bronchoalveolar lavage) Ly6C^{int}Gr1^{hi} neutrophils and Ly6C^{hi} monocytes, and they facilitated the recruitment of neutrophils and monocytes to the airspaces of *E. coli*-injured lungs. Double deletion of *Chrna7* and *Itgam* increased lung recruitment of monocytes and/or neutrophils and deteriorated *E. coli* and LPS-induced lung injury. Thus, signals of vagal circuits engaging with AKT1 in $\alpha 7$ nAChR⁺CD11b⁺ cells attenuate *E. coli* and LPS-induced acute lung inflammatory responses. Targeting this signaling pathway could provide novel therapeutic strategies for treating acute lung injury.

Keywords: Vagal circuits; $\alpha 7$ nicotinic acetylcholine receptor; AKT1; CD11b; acute lung injury

Cell Discovery (2017) 3, 17009; doi:10.1038/celldisc.2017.9; published online 11 April 2017

Introduction

Acute respiratory distress syndrome (ARDS), characterized by acute lung injury (ALI), has a mortality of 30–40%, even if the patients were supported by advanced intensive care [1]. Pneumonia, severe sepsis and acid aspiration are the most serious causes of

ARDS [1–3]. Gram-negative sepsis derived ALI is characterized by neutrophil alveolitis and increased permeability of the lung microvascular endothelial and alveolar epithelial barriers [4–6]. Recruitment of monocytes and neutrophils to the lung is a key event in the propagation of lung inflammation and injury [7, 8].

Cellular and humoral factors could modulate inflammatory responses; however, recent investigations have demonstrated that the inflammatory reflex could regulate innate immune responses as well [9–12]. The vagus nerve, the cranial nerve X, originates from the medullar oblongata, which consists of four nuclei: dorsal nucleus, nucleus ambiguous, nucleus tractus solitarius (NTS) and spinal nucleus of trigeminal

*Correspondence: Michael A Matthay

Tel: +86 021 54923111; Fax: 86-21-54923111;

E-mail: michael.matthay@ucsf.edu

or Xiao Su

Tel: 86-21-54923111; Fax: 86-21-54923111;

E-mail: xsu@ips.ac.cn

Received 8 November 2016; accepted 13 February 2017

nerve [13, 14]. The vagus nerve includes both sensory (afferent) and motor (efferent) fibers [15]. About 80% of the afferent sensory fibers are contained in the vagus nerve and are responsible for transmission of the information to the NTS [13]. The afferent sensory neural arc detects the molecular products of injury, infection and inflammation [16]. The efferent arc transmits action potentials from the NTS to the periphery by the vagus nerve. This process culminates in the release of the neurotransmitter acetylcholine, which interacts with innate immune cells that express the $\alpha 7$ subunit of nicotinic acetylcholine receptor ($\alpha 7$ nAChR) [16]. The afferent and efferent arcs, the information integrating center in the central nervous system, and $\alpha 7$ nAChR-expressing immune cells form an inflammatory reflex [16], which provides the host with a fast, discrete and localized means of controlling the immune responses [9, 17].

It should be emphasized that the vagus nerve ramifies in the celiac ganglion giving rise to the postganglionic splenic nerve that terminates in the spleen. Splenic nerve endings release norepinephrine that activate $\beta 2$ AR (adrenergic receptor)-expressing T memory lymphocytes ($CD4^+CD44^{\text{high}}CD62L^{\text{low}}$) or $CD4^+CHAT^+$ (choline acetyltransferase) cells and initiate synthesis of acetylcholine (ACh) [18]. ACh could activate splenic $\alpha 7$ nAChR-expressing macrophages to inhibit NF- κ B activity and dampen pro-inflammatory cytokine production (especially TNF- α) [18–22]. Therefore, the spleen is the hub of efferent arc of vagal circuits, which forms the cholinergic anti-inflammatory pathway (CAP) [23, 24].

The vagus nerve innervates the distal airway of the lung, especially in the alveoli [25, 26], where sensors or pathogen recognition receptors in the vagal afferent arc may locate. Some airway sensors are predominantly innervated by vagal afferent fibers derived from the nodose ganglion [27]. The information of lung infection and inflammation is transmitted via the afferent arm to the NTS. After integration, the pulmonary vagal nerve endings secrete ACh that can activate $\alpha 7$ nAChR-expressing proinflammatory cells, suppress NF- κ B activation and proinflammatory cytokines, and therefore lessen the extent of lung inflammation and injury [28, 29]. Vagotomy and deficiency of $\alpha 7$ nAChR worsen lipopolysaccharide (LPS) or *Escherichia coli* (*E. coli*)-induced ALI [28, 29]. Thus, pulmonary parasympathetic inflammatory reflexes modulate lung infection and immunity [9, 30, 31].

Vagal circuits could influence trafficking of inflammatory cells via CD11b in the spleen [32]. CD11b is required for adhesion, trafficking, chemotaxis and

phagocytosis of proinflammatory cells [33–40]. Toll-like receptor (TLR)-triggered activation of CD11b integrin inhibits TLR signaling in innate immune responses [41]. AKT1 (serine-threonine protein kinase) is a part of PI3K-dependent signaling pathway involved in multiple cellular responses including survival, growth proliferation and migration [42]. Particularly, AKT1 signaling negatively regulates neutrophil recruitment and activation in ALI [43]. Lung $\alpha 7$ nAChR-expressing $CD11b^+$ and $Gr1^+$ cells are significantly increased during *E. coli* lung infection [29]; but the sources of these cells are elusive. Moreover, the spleen is not only a hub of CAP [18, 23, 24] but also a reservoir of proinflammatory cells (especially, monocytes) [44]. Therefore, we tested whether vagal circuits would regulate spleen release and lung recruitment of $\alpha 7$ nAChR $^+CD11b^+$ cells via phosphorylation of AKT1 by which determined the severity of lung injury.

In this study, we found that disruption of vagal circuit signals promoted splenic release and lung recruitment of $\alpha 7$ nAChR $^+CD11b^+$ cells and reduced *E. coli* and LPS-challenged lung injury. Administration of $\alpha 7$ nAChR agonist PHA568487 to *E. coli* and LPS-challenged vagotomized mice stabilized splenic $\alpha 7$ nAChR $^+CD11b^+$ cells by enhancing phosphorylation of AKT1, reduced lung recruitment of this cell population, and therefore mitigated the severity of lung injury. Deletion of *Akt1* enhanced discharge of splenic $\alpha 7$ nAChR $^+CD11b^+$ cells and lung recruitment of these cells and worsened *E. coli* and LPS-induced lung injury. Double deletion of *Chrna7* and *Itgam* reduced splenic $CD4^+CHAT^+$ cells and phosphorylation of AKT1 in splenic and BAL $ly6C^{\text{hi}}$ monocytes and neutrophils, augmented recruitment of these pro-inflammatory cells to LPS and *E. coli*-challenged lungs, and worsened lung injury. Our findings provide insight into vagal-immune cell regulation of lung inflammatory responses and implicate a therapeutic target for acute lung inflammatory injury.

Results

Disruption of vagal circuits boosts spleen egress and lung recruitment of granulocytes and worsens LPS-induced lung injury

As the hub of CAP [23, 24], spleen is also a reservoir of monocytes, and these cells can be deployed to the inflammatory sites during injury [44]. To test whether the disruption of vagal signals could reduce monocytes in the spleen, while increasing monocytes in the lung in an LPS-induced lung injury mouse model,

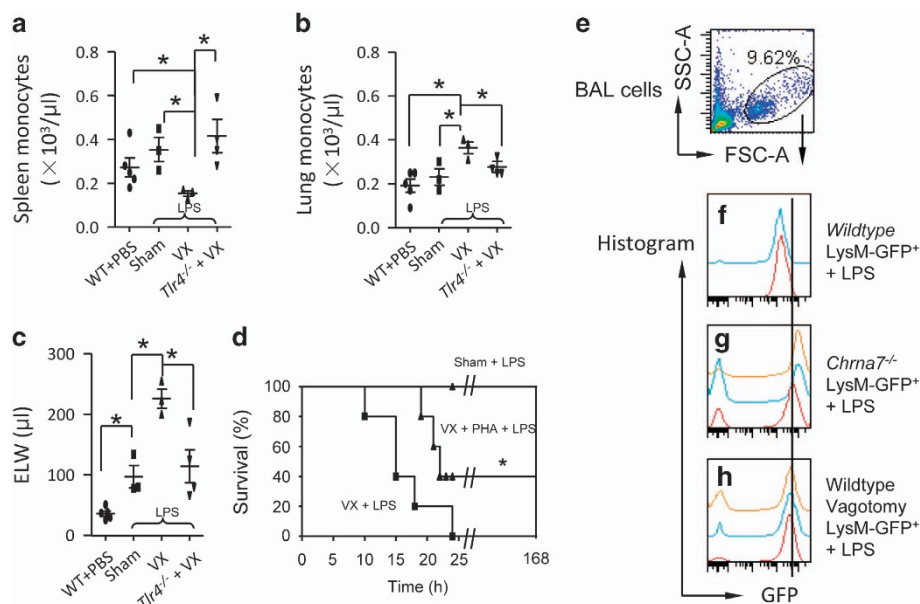


Figure 1 Disruption of vagal circuits exacerbates LPS-induced ALI by enhancing egress of splenic monocytes and migration of granulocytes towards the injured lungs. **(a–c)** Effect of vagotomy on splenic and pulmonary monocytes, and extravascular lung water (ELW) in LPS-induced ALI. The mice were divided into four groups: WT (PBS IT), sham+LPS (5 mg kg⁻¹ IT), vagotomy+LPS (5 mg kg⁻¹ IT) or *Tlr4*^{-/-}+vagotomy+LPS (5 mg kg⁻¹ IT). Mice were killed at 15 h after intratracheal LPS to measure splenic monocytes **(a)**, pulmonary monocytes **(b)** and ELW **(c)**. *N* = 3–5 in each group. Data were pooled from three experiments. **P* < 0.05, one-way ANOVA with Bonferroni *post hoc* test. Data are presented as mean ± s.d. **(d)** Effect of vagotomy on mortality of LPS-induced ALI. The mice were divided into three groups: sham+LPS (*n* = 8), vagotomized+LPS (*n* = 9) and vagotomized+PHA568487+LPS (*n* = 4). The mice were IT instilled with LPS at dose of 5 mg kg⁻¹. Mice of the vagotomized+PHA568487+LPS group were given an intraperitoneal (ip) injection of PHA568487 (0.8 mg kg⁻¹) 15 min before LPS, and repeated the same dose 6, 12 and 18 h, respectively, after LPS to maintain drug concentration in the blood. The corresponding vehicles were given in the other two groups. The mortality of mice was followed up for 7 days. **P* < 0.05 by log-rank test. **(e–h)** Effect of deficiency of $\alpha 7$ nAChR and vagotomy on LysM-GFP⁺ cell migration to the airspaces of the lung during LPS-induced ALI. The mice were divided as follows: wildtype LysM-GFP⁺ mice receiving an IT of LPS (5 mg kg⁻¹), *Chrna7*^{-/-}LysM-GFP⁺ mice receiving an IT of *E. coli* (5 mg kg⁻¹), and vagotomized wildtype LysM-GFP⁺ mice receiving an IT of LPS (5 mg kg⁻¹). The mice were killed at 24 h after LPS challenge. The BAL cells were collected for flow cytometry. The whole-cell population was gated **(e)**. The LysM-GFP histogram was applied to each sample in wildtype LysM-GFP⁺+LPS (*n* = 2) **(f)**, *Chrna7*^{-/-}LysM-GFP⁺+LPS (*n* = 3) **(g)** and vagotomized LysM-GFP⁺+LPS (*n* = 3) **(h)**.

we unilaterally excised the right cervical vagus nerve of mice and then intratracheally (IT) challenged them with LPS. 15 h later, we found that after LPS challenge, vagotomy enhanced the deployment of splenic monocytes (Figure 1a), accumulation of these cells in the lung (Figure 1b) and elevation of extravascular lung water (Figure 1c) compared with the sham mice, which received the same procedures as vagotomy, but the vagus remained intact. Deletion of *Tlr4* in LPS-challenged vagotomized mice reversed these effects (Figure 1a–c), suggesting that vagal signals negatively regulate TLR4 signaling. To show that vagal signals protected LPS-challenged mice via $\alpha 7$ nAChR, we followed up with the LPS-challenged sham and vagotomized mice, and PHA568487 (PHA)-treated LPS-challenged vagotomized mice for

7 days. We found that LPS-challenged sham mice survived for 7 days after LPS; however, the LPS-challenged vagotomized mice died within 25 h. Supplementing with $\alpha 7$ nAChR agonist PHA568487 could rescue 40% of LPS-challenged vagotomized mice during 7 day observation (Figure 1d). In LPS-challenged vagotomized mice, neutrophils were decreased in the spleen (Supplementary Figure S1A), and increased in the peripheral blood (Supplementary Figure S1B) and lungs (Supplementary Figure S1C; MPO, an index of neutrophil infiltration), where pulmonary edema was exacerbated (Supplementary Figure S1D). The p-P65 NF- κ B was increased; however, the p-AKT1^{Ser473} was decreased in the nuclear extract of isolated splenic neutrophils from the LPS-challenged vagotomized mice compared to that

in the LPS-challenged sham mice (Supplementary Figure S1E and F). These findings indicate that splenic neutrophil p-AKT1^{Ser473} might be a negative regulator for lung inflammatory responses. We confirmed that rabbit anti- $\alpha 7$ nAChR antibody could bind $\alpha 7$ nAChR specifically by comparing $\alpha 7$ nAChR⁺ cells between wildtype and *Chrna7*^{-/-} lung, bone marrow (BM) and spleen cells. Fluor-633 α -bungarotoxin labeling in BM cells also proved the specificity of this antibody (Supplementary Figure S2A–G). In the non-LPS challenge condition, vagotomy did not affect percentage of monocytes (Ly6C^{hi}Ly6G^{int}) and neutrophils (Ly6C^{int}Ly6G^{hi}) in the spleen, BM and lung (Supplementary Figure S3A–J).

We used LPS-challenged LysM-GFP⁺ mice (GFP-positive cells are granulocytes [45]) to detect whether vagotomy or deficiency of $\alpha 7$ nAChR could facilitate the recruitment of granulocytes to inflammatory sites. By flow cytometry gating whole BAL cells (Figure 1e), we found that LysM-GFP⁺ granulocytes in the BAL were increased in LPS-challenged LysM-GFP⁺ *Chrna7*^{-/-} or LPS-challenged LysM-GFP⁺ vagotomized mice compared to LPS-challenged LysM-GFP⁺ sham mice at 24 h (Figure 1f–h), suggesting that vagal- $\alpha 7$ nAChR signaling controls the recruitment of granulocytes towards LPS-injured lungs. These findings indicate that vagal signals via $\alpha 7$ nAChR might limit the recruitment of granulocytes to LPS-injured lung and attenuate magnitude of lung injury.

Vagal signals restrain migration of $\alpha 7$ nAChR⁺CD11b⁺ or Gr1⁺ granulocytes towards LPS-injured lung

Splenic $\alpha 7$ nAChR-expressing macrophages can be activated by signals from vagus nerve circuit [9, 10, 18]. Granulocytes express CD11b or Gr1 (marker for neutrophils) [33, 44]. To test whether vagal signals regulate splenic egress and lung recruitment of $\alpha 7$ nAChR⁺CD11b⁺ cells [18], we utilized flow cytometry (Figure 2a, b, d and e). to analyze quantity of $\alpha 7$ nAChR⁺CD11b⁺ cells in the spleen and lung from LPS-induced ALI mice. At 15 h, we found that vagotomy reduced $\alpha 7$ nAChR⁺CD11b⁺ cells in the spleen (Figure 2c), but increased these cells in LPS-challenged lungs (Figure 2f) compared to LPS-challenged sham mice. Deletion of *Tlr4* in LPS-challenged vagotomized mice could invert these events (Figure 2c and f), suggesting that vagal signals regulate flux of $\alpha 7$ nAChR⁺CD11b⁺ cells during LPS-induced ALI depending on TLR4 signaling. To test whether activation of $\alpha 7$ nAChR would mitigate migration of $\alpha 7$ nAChR⁺CD11b⁺ or $\alpha 7$ nAChR⁺Gr1⁺ cells towards LPS-injured airspaces

of the lungs, we pretreated LPS-challenged mice with either saline or $\alpha 7$ nAChR agonists: nicotine, PHA568487 or DMAB. At 24 h, we collected BAL and gated granular cells (Figure 2g and i) and found that the percentage of $\alpha 7$ nAChR⁺CD11b⁺ and $\alpha 7$ nAChR⁺Gr1⁺ cells in the BAL from $\alpha 7$ nAChR agonists-pretreated LPS-challenged mice was reduced compared to saline-pretreated LPS-challenged mice (Figure 2h and j). We pretreated mice with different doses of nicotine or DMAB, and then IT challenged them with LPS. At 24 h, BAL neutrophils were reduced dose-dependently in nicotine or DMAB-treated mice, suggesting that activation of $\alpha 7$ nAChR could limit migration of neutrophils towards the inflamed lungs (Figure 2k). These findings indicate that vagal signals attenuate LPS-induced lung inflammatory responses by limiting lung recruitment of $\alpha 7$ nAChR⁺CD11b⁺ or Gr1⁺ granulocytes.

Vagal signals lessen lung E. coli-induced inflammatory responses by reducing spleen egress and lung recruitment of granulocytes

To determine if vagal signals could lessen *E. coli*-induced lung inflammatory responses by reducing splenic egress and lung recruitment of granulocytes, we divided mice into four groups of mice: normal, sham+*E. coli*, vagotomy+*E. coli* and PHA568487-pretreatment+vagotomy+*E. coli*. The mice were killed at 24 h after IT challenge of *E. coli*. We found that vagotomy decreased monocytes in the spleen (Figure 3a) and elevated these cells in *E. coli*-infected lungs (Figure 3b). Pulmonary edema (Figure 3c), hematocrit (an index of systemic permeability) (Figure 3d), lung *E. coli* colonies (Figure 3e) and CXCL2 levels in supernatant of lung homogenate were all elevated (Figure 3f) in *E. coli*-challenged vagotomized mice compared to *E. coli*-challenged sham mice. However, these effects of vagotomy could be reversed by applying $\alpha 7$ nAChR agonist PHA568487 to the vagotomized animals (Figure 3a–f), suggesting that vagal signals control the flux of splenic monocytes and lung bacterial-induced inflammatory responses dependent on $\alpha 7$ nAChR activation. To further prove that activation of $\alpha 7$ nAChR could reduce the recruitment of granulocytes to *E. coli*-infected lungs, we collected BAL cells from LysM-GFP⁺+*E. coli*, saline-pretreated LysM-GFP⁺+*E. coli*, and PHA568487-pretreated LysM-GFP⁺+*E. coli* groups. At 24 h, we gated live BAL cells (Figure 3g) and found that BAL GFP⁺ granulocytes were increased in saline-pretreated LysM-GFP⁺+*E. coli* group compared to LysM-GFP⁺+*E. coli* group (Figure 3h and i). However, administration of $\alpha 7$

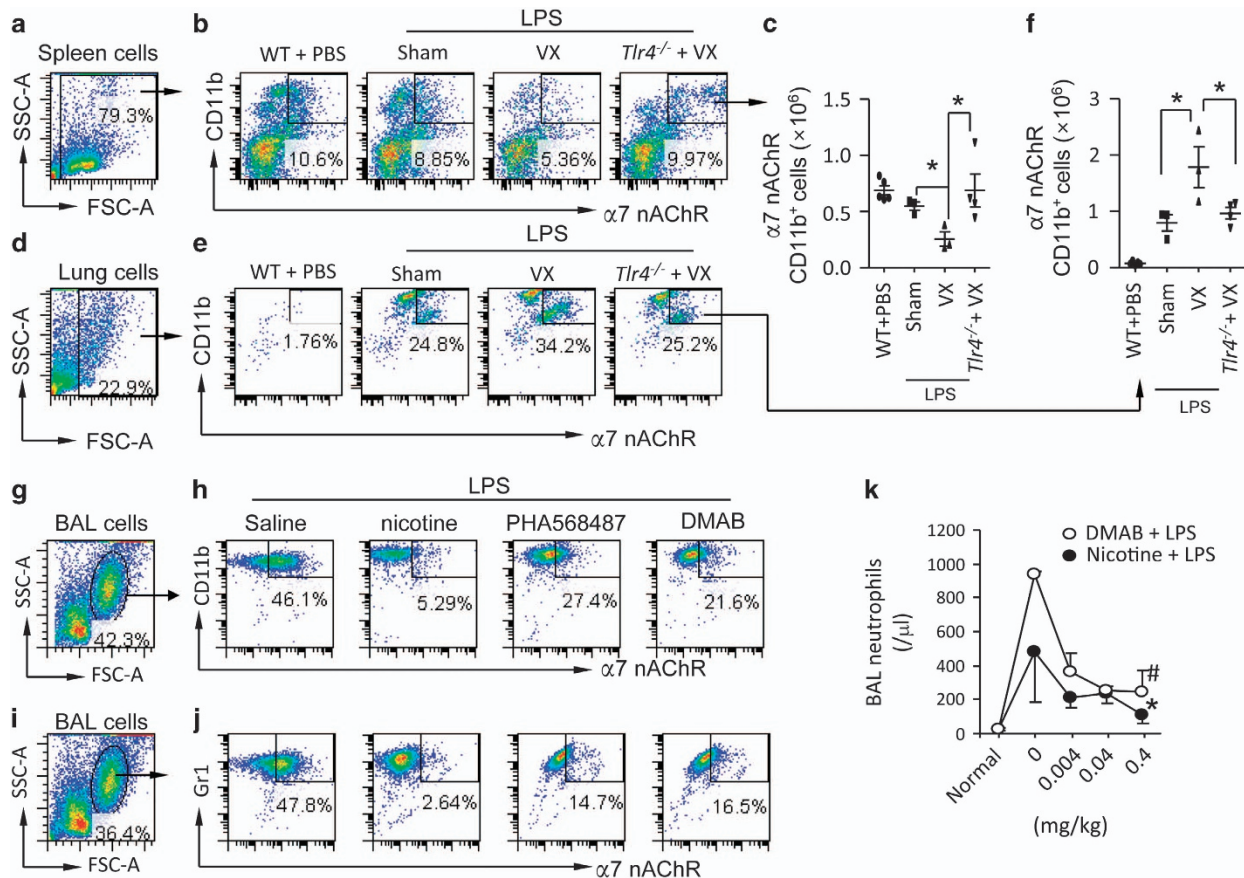


Figure 2 Effect of disruption of vagal circuits and $\alpha 7$ nAChR agonists on $\alpha 7$ nAChR⁺CD11b⁺ cells in the spleen and lung in LPS-induced ALI mouse model. (a–f) Vagotomy affects distribution of $\alpha 7$ nAChR⁺CD11b⁺ cells in the spleen and lung in LPS-induced ALI. The mice were divided into four groups: WT (PBS IT), sham+LPS (5 mg kg⁻¹ IT), vagotomy+LPS (5 mg kg⁻¹ IT) or Tlr4^{-/-}+vagotomy+LPS (5 mg kg⁻¹ IT). Mice were killed at 15 h after LPS instillation. Spleens and lungs were removed to isolate single cells for flow cytometry. The spleen and lung cells were labeled with PE-CD11b and Fluoro-488 $\alpha 7$ nAChR antibodies. The whole live cell population was gated (a, spleen; d, lung). The number of spleen (b) and lung (e) $\alpha 7$ nAChR⁺CD11b⁺ cells was calculated by percentage of cell population multiplied by total cell counts in each spleen or lung (c, f). * $P < 0.05$, between labeled groups. $N = 3–4$ in each group. One-way ANOVA with Bonferroni *post hoc* test. Data are presented as mean \pm s.d. (g–j) Effect of $\alpha 7$ nAChR agonists on the population of $\alpha 7$ nAChR⁺granulocytes in the BAL from LPS-induced ALI. Mice were intraperitoneally pretreated with saline, nicotine (0.4 mg kg⁻¹), PHA568487 (a specific $\alpha 7$ nAChR agonist, 0.4 mg kg⁻¹) or DMAB (a partial $\alpha 7$ nAChR agonist, 0.4 mg kg⁻¹) 15 min before IT of LPS 5 mg kg⁻¹. The saline and $\alpha 7$ nAChR agonists were given every 6 h after LPS. The mice were killed at 24 h after LPS to collect BAL cells for flow cytometry. The BAL cells were labeled with Fluoro-488- $\alpha 7$ nAChR and PE-CD11b or Gr1 antibody. The whole-cell population was selected (g, i) for analyzing $\alpha 7$ nAChR⁺CD11b⁺ cells (h) or $\alpha 7$ nAChR⁺Gr1⁺ cells (j) in the BAL from each group. (k) Effect of nicotine and DMAB on BAL neutrophils in LPS-induced ALI. Mice were intraperitoneally pretreated with saline, nicotine (0.004, 0.04 and 0.4 mg kg⁻¹) or DMAB (0.004, 0.04 and 0.4 mg kg⁻¹) (q6h thereafter, ip) and then received an IT of LPS 5 mg kg⁻¹. The mice were killed at 24 h after LPS to collect BAL cells for measurements. $N = 3–4$ in each group. * $P < 0.05$, # $P < 0.01$, compared with saline-treated group. Data was pooled from two independent experiments. One-way ANOVA with Bonferroni *post hoc* test. Data are presented as mean \pm s.d.

nAChR agonist PHA568487 in LysM-GFP⁺+*E. coli* group reduced BAL GFP⁺ granulocytes compared to saline-pretreated LysM-GFP⁺+*E. coli* group (Figure 3i and j), supporting the conclusion that vagal signals reduce lung recruitment of granulocytes in *E. coli*-challenged lungs via $\alpha 7$ nAChR activation.

Vagal signals via serine473 phosphorylation of AKT1 limit discharge of $\alpha 7$ nAChR⁺CD11b⁺ cells from spleen and suppress recruitment of these cells to the injured lung

We performed lung immunofluorescence and found that $\alpha 7$ nAChR⁺ and $\alpha 7$ nAChR⁺Gr1⁺ cells were increased in *E. coli*-infected vagotomized mice

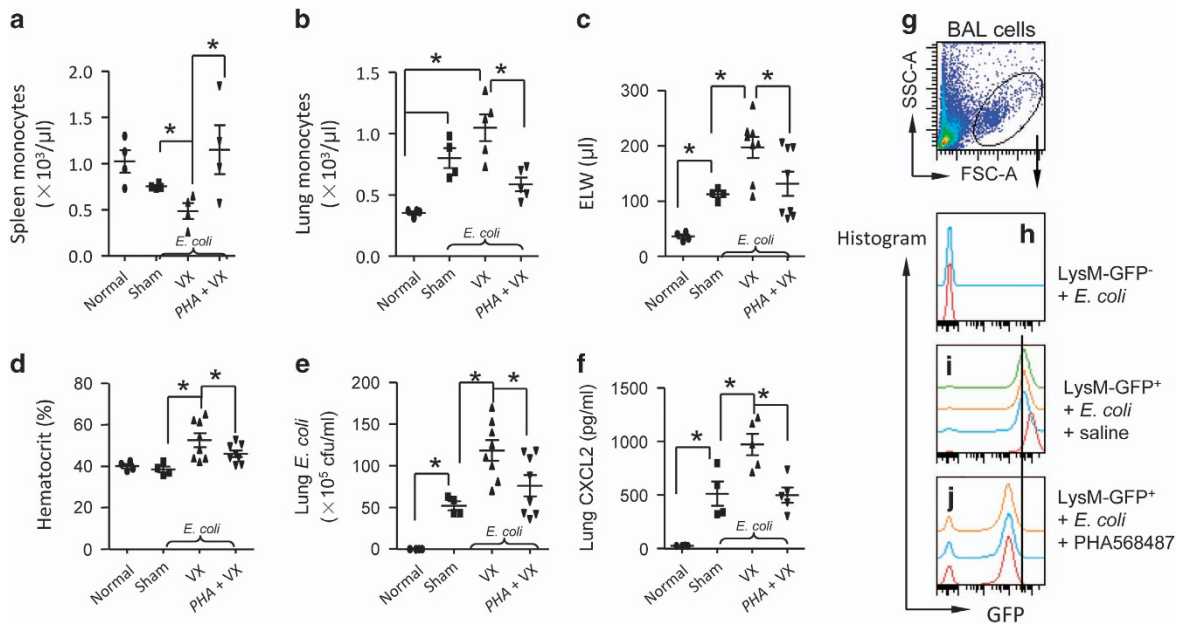


Figure 3 Disruption of vagal circuits exacerbates *E. coli*-induced ALI by enhancing migration of granulocytes towards the injured lungs. (a–d) Vagal- $\alpha 7$ nAChR signaling regulates quantity of splenic and lung monocytes, pulmonary edema, severity of lung infection and chemokine levels in *E. coli* pneumonia. Mice were randomly divided into four groups: Normal, sham+ *E. coli*, vagotomized+*E. coli* and vagotomized+PHA568487 (PHA)+*E. coli*. Normal controls were naive mice. Sham+*E. coli* and vagotomized+*E. coli* received an IT of *E. coli* (2.5×10^6) and corresponding vehicle treatment. The vagotomized+PHA+*E. coli* group received an IP of PHA (0.4 mg kg^{-1}) 15 min prior to intratracheal *E. coli* (2.5×10^6). The PHA therapy was given IP every 6 h. The mice were killed 24 h later to measure number of splenic (a) and lung monocytes (b), ELW (c), hematocrit (d), *E. coli* colonies (e) and CXCL2 (a chemokine of neutrophils) (f) in the supernatants of lung homogenates. $*P < 0.05$, compared with the indicated group. Data was pooled from two independent experiments. (g–j) Effect of activation of $\alpha 7$ nAChR on migration of granulocytes towards the injured lungs during *E. coli* pneumonia. The mice were divided as follows: LysM-GFP⁻ mice receiving an IT of *E. coli* (2.5×10^6 cfu), LysM-GFP⁺ mice receiving an IT of *E. coli* (2.5×10^6 cfu), and LysM-GFP⁺ mice pretreated with PHA568487 (a specific $\alpha 7$ nAChR agonist, 0.4 mg kg^{-1} , given IP every 6 h), and received an IT of *E. coli* (2.5×10^6 cfu). The mice were killed at 24 h after *E. coli* infection. The BAL cells were collected for flow cytometry. The whole-cell population was gated (g). The LysM-GFP histogram was applied to each sample in LysM-GFP⁺ + *E. coli* ($n = 2$) (h), LysM-GFP⁺+*E. coli* ($n = 4$) (i) and LysM-GFP⁺+*E. coli*+PHA568487 ($n = 3$) (j).

compared to *E. coli*-infected sham mice 12 and 24 h after IT challenge of *E. coli* (Supplementary Figure S4A and B). This finding supports that vagal signals regulate recruitment of $\alpha 7$ nAChR⁺ granulocytes to *E. coli*-infected lung. To clarify the underlying mechanism that defines the movement of $\alpha 7$ nAChR⁺ granulocyte, we isolated spleen, peripheral blood and lung cells from normal, sham+*E. coli*, vagotomy+*E. coli*, and PHA568487-pretreatment+vagotomy+*E. coli* mice to analyze $\alpha 7$ nAChR⁺CD11b⁺ cells and serine473 phosphorylation of AKT1 24 h after *E. coli* challenge (Figure 4a, b and d). We found that splenic $\alpha 7$ nAChR⁺CD11b⁺ cells were markedly decreased in *E. coli*-infected vagotomized mice compared with *E. coli*-infected sham mice (Figure 4c); furthermore, p-AKT1^{Ser473}+ $\alpha 7$ nAChR⁺CD11b⁺ cells were declined in *E. coli*-infected vagotomized mice compared to

E. coli-infected sham mice (Figure 4e). The above changes were reversed if administrating $\alpha 7$ nAChR agonist PHA568487 to the vagotomized mice (Figure 4c and e). These findings indicate that serine473 phosphorylation of AKT1 in $\alpha 7$ nAChR⁺CD11b⁺ cells suppress exit of these cells from spleen. By separately analyzing lymphocyte (L), monocyte (M) and polymorphonuclear leukocyte gates (Supplementary Figure S5A, D and G) in peripheral blood cells from these four groups of mice (Supplementary Figure S5B, E and H), we found that there were more blood $\alpha 7$ nAChR⁺CD11b⁺ cells in *E. coli*-infected vagotomized mice than *E. coli*-infected sham mice; however, this change was counteracted by activation of $\alpha 7$ nAChR (Supplementary Figure S5C, F and I). We gated the $\alpha 7$ nAChR⁺CD11b⁺ population from lung cells (Figure 4f and g) and found that $\alpha 7$ nAChR⁺CD11b⁺ cells were

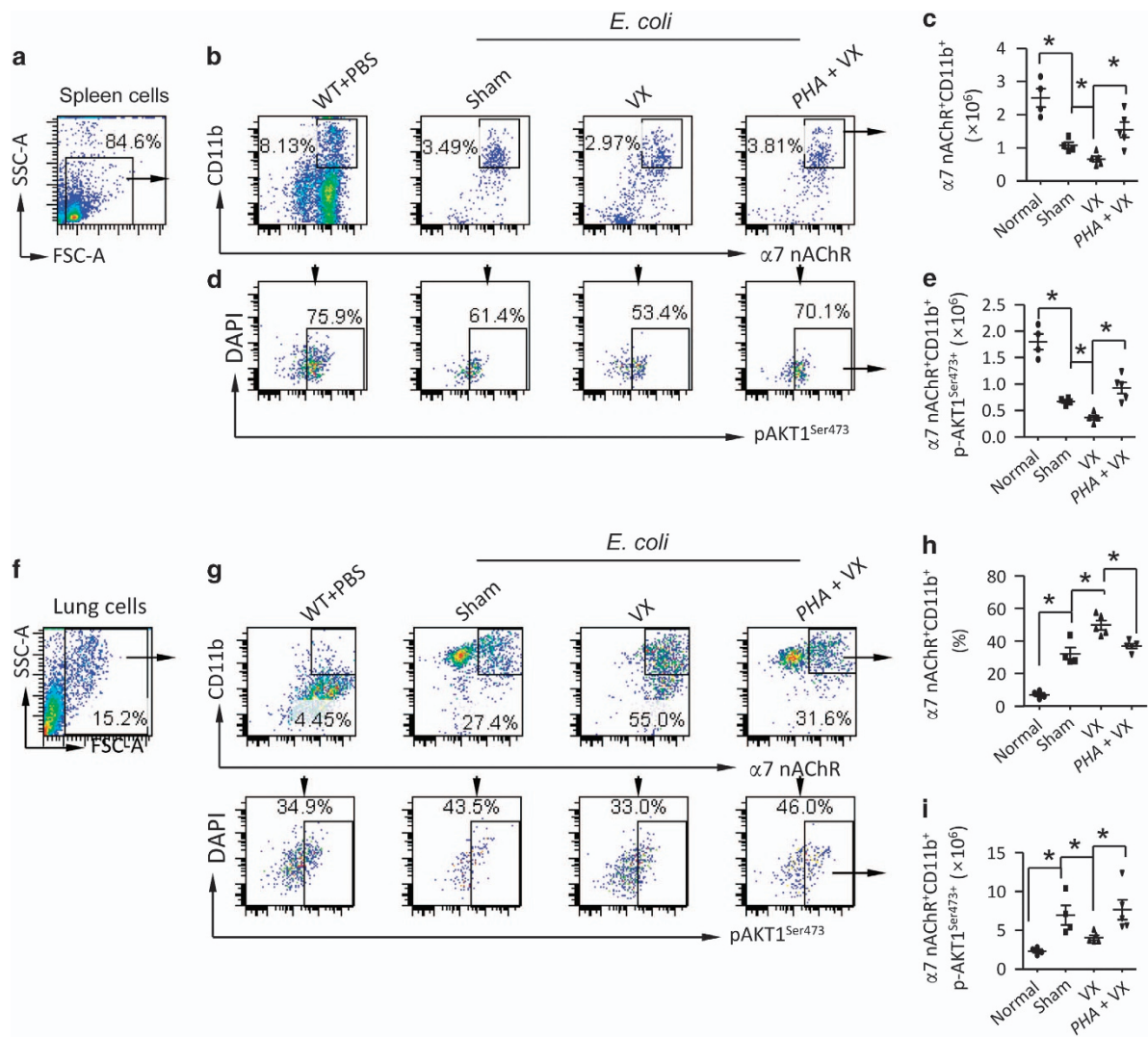


Figure 4 Vagal- $\alpha 7$ nAChR signaling engages with phosphorylation of AKT1^{Ser473+} to prevent egress of $\alpha 7$ nAChR⁺CD11b⁺ cells from spleen and recruitment of these cells towards *E. coli*-injured lungs. (a–e) Vagal- $\alpha 7$ nAChR signaling regulates of p-AKT1^{Ser473+} in splenic $\alpha 7$ nAChR⁺CD11b⁺ cells during *E. coli* pneumonia. Sham, vagotomized and vagotomized plus PHA568487 (0.4 mg kg⁻¹ pretreated 15 min prior to *E. coli* (2.5 × 10⁶ cfu) and given every 6 h, IP). The mice were killed 24 h after infection. The spleen cells were collected and labeled with the indicated fluorescent antibodies. The granular cells were gated (a). The $\alpha 7$ nAChR⁺CD11b⁺ cells were first analyzed and then calculated the percentage of p-AKT1^{Ser473+} cells (b–e). *N* = 4–5 in each group. **P* < 0.05, one-way ANOVA with Bonferroni *post hoc* test. (f–i) Flow cytometry analysis of $\alpha 7$ nAChR⁺CD11b⁺ cell population the lung during *E. coli* pneumonia. Using the same experimental setting as (a–e), the lung cells were collected and labeled with the indicated fluorescent antibodies. The granular cells were gated (f). The $\alpha 7$ nAChR⁺CD11b⁺ cells and $\alpha 7$ nAChR⁺CD11b⁺ p-AKT1^{Ser473+} cells were analyzed (g). The percentage of $\alpha 7$ nAChR⁺CD11b⁺ cells and number of $\alpha 7$ nAChR⁺CD11b⁺ p-AKT1^{Ser473+} cells were calculated (h, i). *N* = 4–5 in each group. **P* < 0.05, one-way ANOVA with Bonferroni *post hoc* test. Data are presented as mean ± s.d.

increased in *E. coli*-infected vagotomized lung compared to relative to *E. coli*-infected sham lung; administrating $\alpha 7$ nAChR agonist PHA568487 corrected this change (Figure 4h). The number of lung p-AKT1^{Ser473+} $\alpha 7$ nAChR⁺CD11b⁺ cells was reduced in *E. coli*-infected vagotomized mice compared with *E. coli*-infected sham mice, and activation of $\alpha 7$

nAChR in *E. coli*-infected vagotomized mice restored this change (Figure 4i). The findings indicate that vagal- $\alpha 7$ nAChR signal via phosphorylation of AKT1 at serine73 site stabilizes $\alpha 7$ nAChR⁺CD11b⁺ cells in the spleen and prevents these cells from migrating to peripheral blood and *E. coli*-infected lung. To demonstrate that activation of $\alpha 7$ nAChR induces

AKT1 phosphorylation, which suppresses proinflammatory responses, we pretreated wildtype and *Chrna7*^{-/-} splenic neutrophils with $\alpha 7$ nAChR specific agonist PHA568487 and then challenged them with LPS and separated cytoplasm and nucleus 1 h later. Activation of $\alpha 7$ nAChR promoted phosphorylation of p-AKT1 at Ser473 site in splenic neutrophil cytoplasm (Supplementary Figure S6A), but reduced it in the nucleus (Supplementary Figure S6B). Activation of $\alpha 7$ nAChR also suppressed CXCL2 production in LPS-challenged splenic neutrophils (Supplementary Figure S6C). Inhibition of phosphorylation of AKT1 by Wortmannin increased CXCL2 production in LPS-challenged splenic neutrophils (Supplementary Figure S6D). Deletion of *Itgam* increased CXCL2 and TNF- α production in LPS-challenged splenic neutrophils (Supplementary Figure S6E). These findings provide evidence that $\alpha 7$ nAChR-p-AKT1 signaling negatively regulates proinflammatory responses in neutrophils.

Deletion of Akt1 enhances spleen egress and lung recruitment of $\alpha 7$ nAChR⁺CD11b⁺ cells and deteriorates lung injury

To investigate whether deletion of *Akt1* could enhance splenic release of $\alpha 7$ nAChR⁺CD11b⁺ cells, we isolated spleen cells from *E. coli*-infected wildtype and *Akt1*^{-/-} mice 24 h after IT *E. coli*. The spleen/body weight ratio in *E. coli*-infected *Akt1*^{-/-} mice was lower than *E. coli*-infected wildtype mice (Figure 5a). We gated $\alpha 7$ nAChR⁺CD11b⁺ cell population in spleen cells (Figure 5b and c) and found that the number of splenic $\alpha 7$ nAChR⁺CD11b⁺ cells was lower in *E. coli*-infected *Akt1*^{-/-} mice than *E. coli*-infected wildtype mice (Figure 5d). The number of spleen neutrophils was also lower in *E. coli*-infected *Akt1*^{-/-} mice (Figure 5e). In lung cells (Figure 5f), percentage (Figure 5g) and absolute number (Figure 5h) of $\alpha 7$ nAChR⁺CD11b⁺ cells were higher in *E. coli*-infected *Akt1*^{-/-} mice than *E. coli*-infected wildtype mice. Lung neutrophils (Figure 5i) and TNF- α (Figure 5j) in *E. coli*-infected *Akt1*^{-/-} mice were elevated compared to *E. coli*-infected wildtype mice. To study whether deletion of *Akt1* would facilitate recruitment of $\alpha 7$ nAChR⁺CD11b⁺ and $\alpha 7$ nAChR⁺Gr1⁺ cells to *E. coli*-infected lung, we IT challenged wildtype and *Akt1*^{-/-} mice with *E. coli* and killed them at d1, d2 and d3. The BAL cells were isolated to analyze $\alpha 7$ nAChR⁺CD11b⁺ and $\alpha 7$ nAChR⁺Gr1⁺ cells (Figure 5k–m). The percentage of BAL $\alpha 7$ nAChR⁺CD11b⁺ and $\alpha 7$ nAChR⁺Gr1⁺ cells was increased in *E. coli*-infected *Akt1*^{-/-} mice compared to *E. coli*-infected wildtype

mice (Figure 5k–m). In an LPS-induced ALI mouse model, BAL neutrophils and protein levels were higher in LPS-challenged *Akt1*^{-/-} mice compared to LPS-challenged wildtype mice (Figure 5n and o). We also IT challenged wildtype and *Akt1*^{-/-} mice with *E. coli* to study BAL profiles. At 24 h, we found that BAL protein (Supplementary Figure S7A), *E. coli* colonies (Supplementary Figure S7B) and TNF- α (Supplementary Figure S7C) were higher in *E. coli*-infected *Akt1*^{-/-} mice than *E. coli*-infected wildtype mice. The findings strongly support that deletion of *Akt1* enhances splenic release of $\alpha 7$ nAChR⁺CD11b⁺ cells, facilitates migration of these cells towards *E. coli* and LPS-challenged lung, and propagates lung injury.

Deletion of Chrna7 reduces phosphorylation of AKT1^{Ser473} which facilitates splenic egress and lung recruitment of CD11b⁺ cells towards E. coli-infected lung

In *E. coli* pneumonia, *E. coli*-infected *Chrna7*^{-/-} or vagotomized mice had higher BAL protein (Supplementary Figure S8A), *E. coli* colonies (Supplementary Figure S8B) and TNF- α (Supplementary Figure S8C), and they had less splenic p-AKT1^{Ser473}, p-STAT3 and p-ERK (Supplementary Figure S8D–F), suggesting that AKT1 is in the downstream of vagal- $\alpha 7$ nAChR signaling. To verify this, we isolated the spleen (Figure 6a and b) and lung cells (Figure 6d and e) from *E. coli*-infected wildtype and *Chrna7*^{-/-} mice. By flow cytometry analysis, we found that the percentage of p-AKT1^{Ser473} expressing cells in both the spleen (Figure 6c) and lung (Figure 6f) from *E. coli*-infected *Chrna7*^{-/-} mice was decreased compared to that from *E. coli*-infected wildtype mice. The lower phosphorylation of serine473 AKT1 was associated with higher levels of lung neutrophils (Figure 6g) and *E. coli* colonies (Figure 6h) compared to wildtype. This finding supports the conclusion that $\alpha 7$ nAChR via phosphorylation of AKT1 regulates neutrophil migration and bacterial growth. Next, we tested whether the deletion of *Chrna7* would affect the distribution of CD11b⁺ cells between the spleen and the lung during *E. coli* infection. We separately IT challenged wildtype, *Chrna7*^{-/-}, *Akt1*^{-/-} and *Itgam*^{-/-} mice with *E. coli* and isolated splenic cells at 24 h. The granular cells were gated (Figure 6i) and CD11b⁺ cells were subgated in each group (Figure 6j). The percentage of CD11b⁺ cells was decreased in *E. coli*-infected *Chrna7*^{-/-} and *Akt1*^{-/-} spleens compared to *E. coli*-infected wildtype spleen (Figure 6k), suggesting that $\alpha 7$ nAChR and AKT1 are important for controlling egress of splenic CD11b⁺ cells. We also isolated BAL cells from *E. coli*-infected

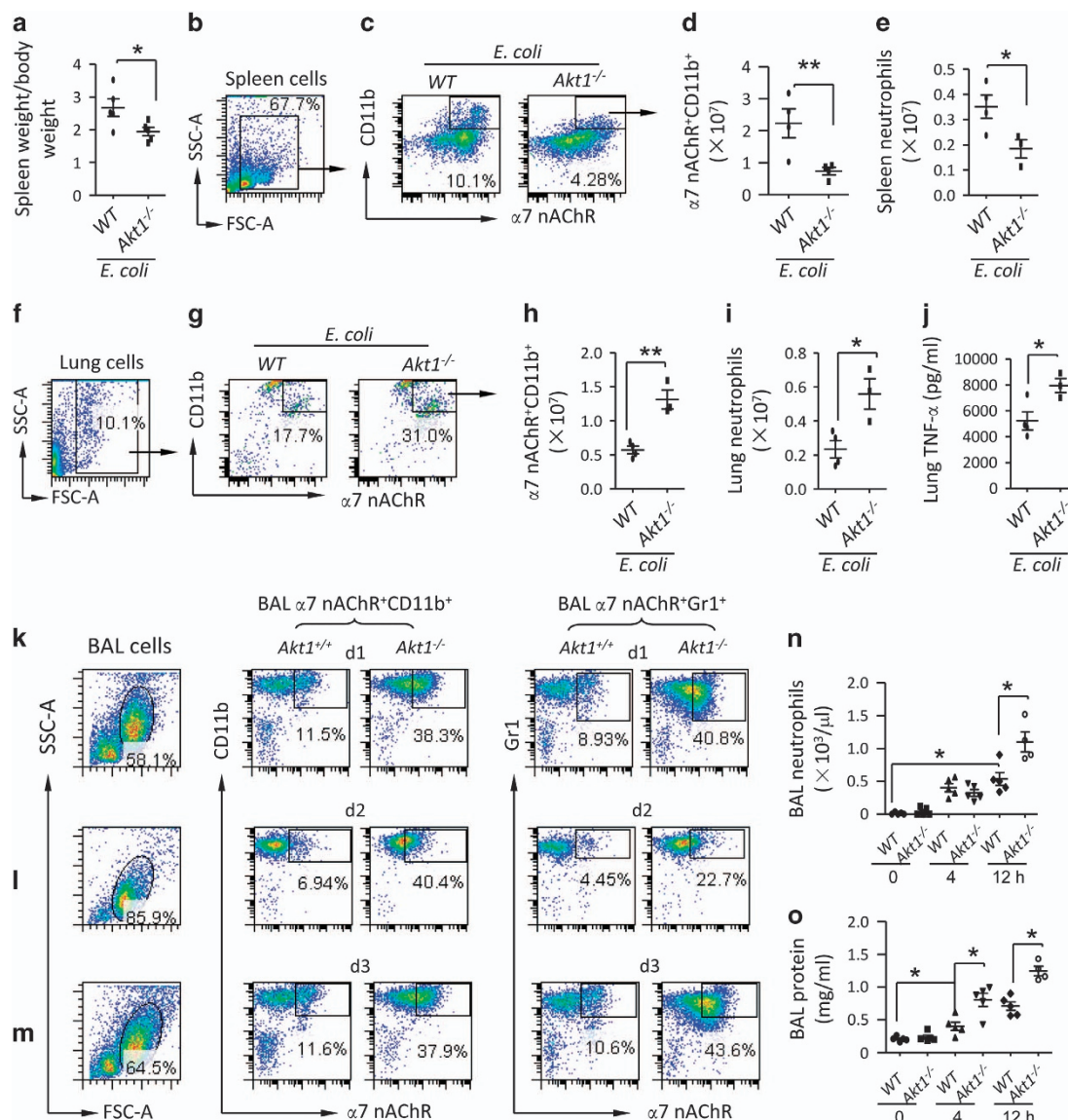


Figure 5 Deficiency of AKT1 facilitates release of $\alpha 7$ nAChR⁺CD11b⁺ cells from spleen and recruitment of these cells to the injured lungs. (**a–e**) Deficiency of AKT1 reduces splenic $\alpha 7$ nAChR⁺CD11b⁺ cells. The wildtype and Akt1^{-/-} mice were challenged with an IT of *E. coli* (2.5×10^6 cfu), and were killed 24 h later. The spleen/body weight ratio was compared (**a**). The spleen cells were labeled with anti- $\alpha 7$ nAChR and CD11b fluorescent antibodies. The whole-cell population was gated to analyze $\alpha 7$ nAChR⁺CD11b⁺ cell population (**b, c**). The percentage multiplied counts of splenocytes to obtain absolute number of $\alpha 7$ nAChR⁺CD11b⁺ cells (**d**). Spleen neutrophils were counted by Wright's staining (**e**). $N = 3-4$ in each group. * $P < 0.05$, ** $P < 0.01$, Student's *t*-test. Data are presented as mean \pm s.d. (**f–j**) Deficiency of AKT1 enhances recruitment of $\alpha 7$ nAChR⁺CD11b⁺ cells and neutrophils to the lung and lung TNF- α level. The lung cells were labeled with anti- $\alpha 7$ nAChR and CD11b fluorescent antibodies. The whole-cell population was gated to analyze $\alpha 7$ nAChR⁺CD11b⁺ cell population (**f, g**). The percentage multiplied counts of splenocytes to obtain absolute number of $\alpha 7$ nAChR⁺CD11b⁺ cells (**h**). Lung neutrophils were counted by Wright's staining (**i**) and TNF- α levels were measured by ELISA (**j**). $N = 3-4$ in each group. * $P < 0.05$, Student's *t*-test. Data are presented as mean \pm s.d. (**k–m**) Effect of deficiency of Akt1 on $\alpha 7$ nAChR⁺CD11b⁺ and $\alpha 7$ nAChR⁺Gr1⁺ cell population in the BAL during *E. coli* pneumonia. The wildtype and Akt1^{-/-} mice were challenged with an IT of *E. coli* (2.5×10^6 cfu). The mice were killed at d 1, 2 and 3 after *E. coli* challenge. The BAL was collected to harvest BAL cells for flow analysis. The cells were labeled with anti- $\alpha 7$ nAChR, CD11b and Gr1 fluorescent antibodies. The whole-cell population was gated. $\alpha 7$ nAChR⁺CD11b⁺ and $\alpha 7$ nAChR⁺Gr1⁺ cells were analyzed at d 1 (**k**), d 2 (**l**) and d 3 (**m**) in the BAL cells. (**n, o**) Effect of deficiency of AKT1 on BAL neutrophils and protein in LPS-induced ALI. Wildtype and Akt1-deleted mice were IT challenged with LPS (5 mg kg^{-1}). The mice were killed at 4 and 12 h after LPS challenge. BAL was collected to measure neutrophil count (**n**) and protein levels (**o**). $N = 4-5$ in each group. * $P < 0.05$, Student's *t*-test. Data are presented as mean \pm s.d.

wildtype and *Chrna7*^{-/-} mice at 24 h. The BAL cells were labeled with anti-CCR2 (a chemokine receptor of MCP-1, which has a role in chemotaxis of monocytes) and CD11b fluorescent antibodies. The granular cells were separately gated (Figure 6l) and CCR2⁺CD11b⁺ cells were subgated in wildtype and *Chrna7*^{-/-} cells (Figure 6m). The percentage of CCR2⁺CD11b⁺ cells was increased in the *E. coli*-infected *Chrna7*^{-/-} BAL compared to *E. coli*-infected wildtype BAL (Figure 6n). These findings support that $\alpha 7$ nAChR via downstream AKT1 regulates spleen egress and lung recruitment of CD11b⁺ cells. Furthermore, we tested whether the deletion of *Akt1* could simulate deletion of *Chrna7* to deteriorate *E. coli* and LPS-induced ALI. We found that ELW (Supplementary Figure S9A), blood neutrophils and monocytes (Supplementary Figure S9B and C), and lung MPO activity (Supplementary Figure S9D) were increased in *E. coli*-infected *Akt1* and *Chrna7*-deleted mice compared with *E. coli*-infected wildtype counterparts. Higher mortality was found in *E. coli*-infected *Akt1* and *Chrna7*-deleted mice compared with *E. coli*-infected wildtype mice (Supplementary Figure S9E). The findings suggest that vagal- $\alpha 7$ nAChR-p-AKT1 signaling negatively regulates egress of splenic CD11b⁺ cells and the severity of *E. coli* and LPS-induced lung inflammatory injury.

Vagotomy and double deletion of Chrna7 and Itgam reduce splenic ly6C^{int}Gr1^{hi} and ly6C^{hi}p-AKT1^{ser473+} and CD4⁺CHAT⁺ ACh-producing cells

Because vagal signals stabilize $\alpha 7$ nAChR⁺CD11b⁺ cells in the spleen via phosphorylation of AKT1, we tested whether vagotomy or double deletion of *Chrna7* and *Itgam* could reduce p-AKT1^{ser473+} in splenic ly6C^{int}Gr1^{hi} neutrophils and ly6C^{hi} monocytes. We IT challenged sham, vagotomized and *Chrna7*^{-/-}*Itgam*^{-/-} mice with *E. coli*. At 24 h, spleen cells were isolated and subjected to flow cytometry. Cells were gated (Figure 7a and e) and ly6C^{int}Gr1^{hi} neutrophils and ly6C^{hi} monocytes were subgated (Figure 7b and f) to analyze percentage of p-AKT1^{ser473+} cells. The percentage of ly6C^{int}Gr1^{hi} neutrophils and ly6C^{hi} monocytes in *E. coli*-infected vagotomized and *Chrna7*^{-/-}*Itgam*^{-/-} mice was reduced compared to *E. coli*-infected sham mice (Figure 7c and g). Also, the percentage of p-AKT1^{ser473+} population in the ly6C^{int}Gr1^{hi} neutrophils and ly6C^{hi} monocytes was decreased in *E. coli*-infected vagotomized and *Chrna7*^{-/-}*Itgam*^{-/-} mice compared to *E. coli*-infected sham mice (Figure 7d and h). These findings indicate that vagal signals reduce spleen egress of neutrophils and monocytes via serine phosphorylation of AKT1. Considering that CD4⁺CHAT⁺

ACh-producing cells relay vagal outflow at spleen nerve terminus [18], we repeated experiment as Figure 7a–d at 24 h. Lymphocytes in splenic cells were gated (Figure 7i) and CD4⁺CHAT⁺ cells were subgated in normal, *E. coli*-infected sham, vagotomized, and *Chrna7*^{-/-}*Itgam*^{-/-} groups (Figure 7j). The percentage and number of splenic CD4⁺CHAT⁺ cells in *E. coli*-infected vagotomized and *Chrna7*^{-/-}*Itgam*^{-/-} mice were significantly reduced compared to *E. coli*-infected sham mice (Figure 7k and l). The percentage of splenic CD4⁺ cells in *E. coli*-infected vagotomized and *Chrna7*^{-/-}*Itgam*^{-/-} mice were decreased relative to *E. coli*-infected wildtype mice (Supplementary Figure S10A and B). Western blotting showed that splenic p-AKT1 and CHAT expression was reduced in *Chrna7*^{-/-}*Itgam*^{-/-} mice compared with *E. coli*-infected wildtype mice (Supplementary Figure S10C and D). These findings suggest that the reduction of CD4⁺CHAT⁺ cells might contribute to less serine473 phosphorylation of AKT1 in the vagotomized and *Chrna7*^{-/-}*Itgam*^{-/-} mice.

Defect of Serine473 phosphorylation of AKT1 in BAL neutrophils and monocytes from E. coli-infected vagotomized or Chrna7^{-/-}Itgam^{-/-} mice

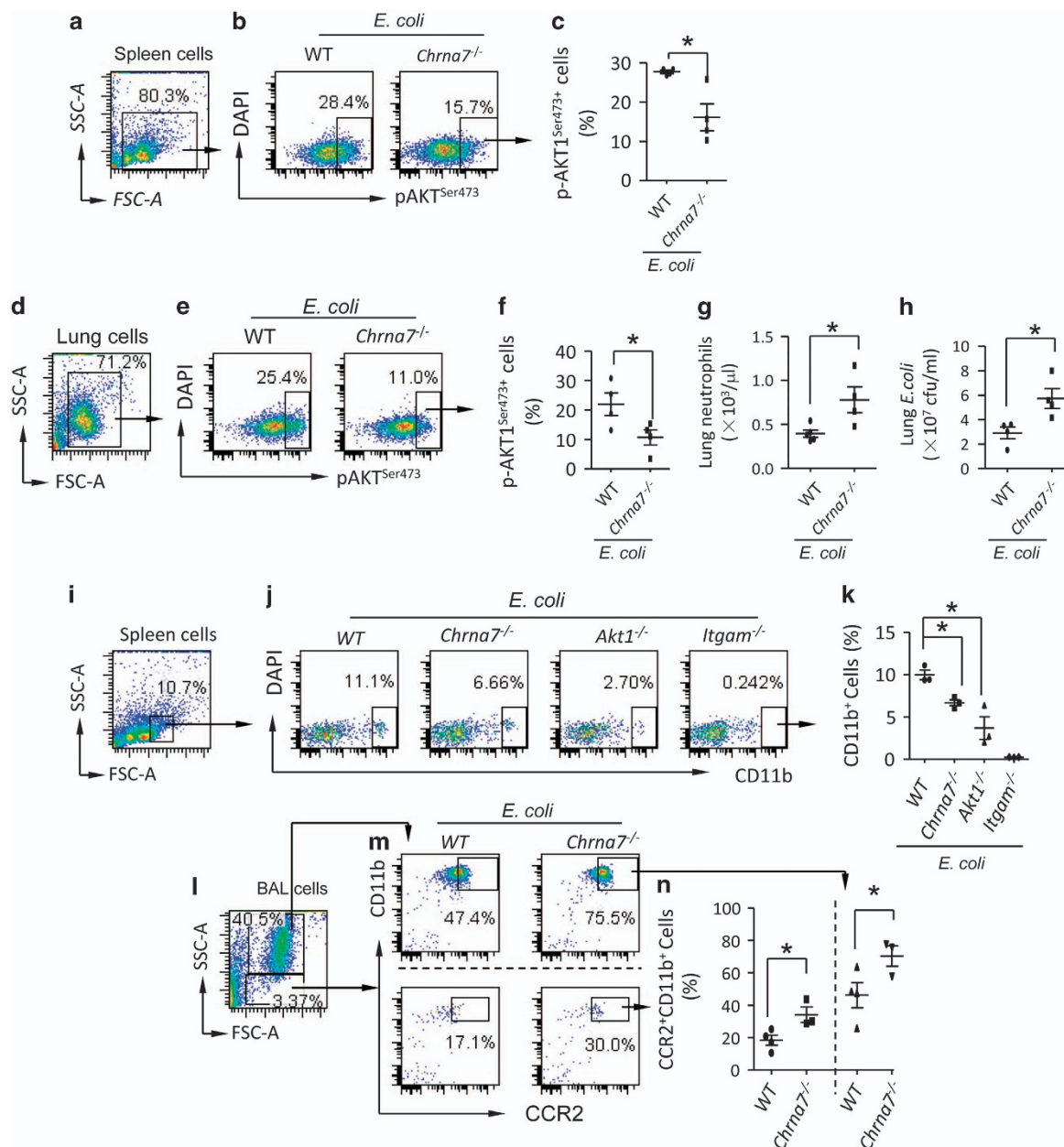
To test whether vagotomy or double deletion of *Chrna7* and *Itgam* impaired serine473 phosphorylation of AKT1 in recruited neutrophils and monocytes during *E. coli* infection, we IT challenged sham, vagotomized and *Chrna7*^{-/-}*Itgam*^{-/-} mice with *E. coli*. At 24 h, BAL cells were isolated and subjected to flow cytometry. To analyze serine473 phosphorylation of AKT1 in BAL neutrophils, we first gated the whole-cell population (Figure 8a) and subgated the ly6C^{int}Gr1^{hi} neutrophils in each group (Figure 8b). The percentage of p-AKT1^{ser473+} population was calculated from ly6C^{int}Gr1^{hi} cells. We found that the percentage of ly6C^{int}Gr1^{hi} neutrophils in BAL from *E. coli*-infected vagotomized or *Chrna7*^{-/-}*Itgam*^{-/-} mice was increased compared to *E. coli*-infected sham mice (Figure 8c). The percentage of p-AKT1^{ser473+} population in ly6C^{int}Gr1^{hi} neutrophils in BAL from *E. coli*-infected vagotomized or *Chrna7*^{-/-}*Itgam*^{-/-} mice was decreased compared to *E. coli*-infected sham mice (Figure 8d). The histology of isolated BAL cells also showed the number of neutrophils was markedly higher in the *E. coli*-infected vagotomized or *Chrna7*^{-/-}*Itgam*^{-/-} mice (Figure 8e). Using the same gating strategies (Figure 8f and g), we found that the percentage of ly6C^{hi} monocytes in BAL from *E. coli*-infected vagotomized or *Chrna7*^{-/-}*Itgam*^{-/-} mice was increased compared to *E. coli*-infected sham mice (Figure 8h).

The percentage of p-AKT1^{Ser473+} population in Ly6C^{hi} monocytes in BAL from *E. coli*-infected vagotomized or *Chrna7*^{-/-}*Itgam*^{-/-} mice was decreased compared to *E. coli*-infected sham mice (Figure 8i). We used the same experimental setting and found that lung *Il22* mRNA was reduced and *Cxcl2* mRNA was increased in *E. coli*-infected vagotomized or *Chrna7*^{-/-}*Itgam*^{-/-} mice (Supplementary Figure S11A and B). BM monocytes (Ly6C^{hi}Ly6G^{int}) in *E. coli*-infected vagotomized and *Chrna7*^{-/-}*Itgam*^{-/-} mice were increased compared to *E. coli*-infected wildtype mice, whereas BM neutrophils (Ly6C^{int}Ly6G^{hi}) were not different among these three groups (Supplementary

Figure S11C–E). These findings indicate that vagal signals regulate splenic neutrophils and monocytes to the infected lungs via serine phosphorylation of AKT1.

Deletion of *Itgam* or *Chrna7* worsens *E. coli* and LPS-induced ALI

Peritoneal macrophages were isolated from wildtype, *Chrna7*^{-/-}, *Itgam*^{-/-} and *Chrna7*^{-/-}*Itgam*^{-/-} mice, and stimulated with LPS for 4 h. TNF- α in the supernatant of culture media was significantly increased in LPS-challenged *Chrna7*^{-/-}, *Itgam*^{-/-} and *Chrna7*^{-/-}*Itgam*^{-/-} macrophages (Supplementary Figure S12). We tested



whether deletion of *Itgam* or/and *Chrna7* would worsen *E. coli* pneumonia. To this end, we IT challenged mice with WT, *Chrna7*^{-/-}, *Itgam*^{-/-} and *Chrna7*^{-/-}*Itgam*^{-/-} mice with *E. coli*. We found that ELW (Figure 9a), CXCL2 (Figure 9b), *E. coli* colonies (Figure 9c), neutrophils and monocytes (Figure 9d and e) in the lungs were increased in *E. coli*-infected *Chrna7*^{-/-}, *Itgam*^{-/-} and *Chrna7*^{-/-}*Itgam*^{-/-} groups compared with *E. coli*-infected WT group. We also collected BAL in *E. coli* pneumonia and found that BAL *E. coli* colonies (Figure 9f), protein (Figure 9g) and TNF- α level (Figure 9h) were increased in *E. coli*-infected *Itgam*^{-/-} and *Chrna7*^{-/-}*Itgam*^{-/-} groups compared with *E. coli*-infected WT group.

To study whether deletion of *Itgam* or/and *Chrna7* would exacerbate LPS-induced ALI, we IT challenged wildtype, *Itgam*^{-/-} and *Chrna7*^{-/-}*Itgam*^{-/-} mice with LPS. There were more severe pulmonary edema (Figure 9i) and higher lung TNF- α (Figure 9j) and monocytes (Figure 9k) in LPS-challenged *Itgam*^{-/-} and *Chrna7*^{-/-}*Itgam*^{-/-} mice compared with the LPS-challenged WT group; however, these parameters were not different between the LPS-challenged *Itgam*^{-/-} group and *Chrna7*^{-/-}*Itgam*^{-/-} group (Figure 9i–k). These findings support that $\alpha 7$ nAChR⁺CD11b⁺ cells have a protective role during *E. coli* and LPS-induced lung injury.

Discussion

$\alpha 7$ nAChR-expressing macrophages and CD4⁺ CHAT⁺ cells in the spleen are the effector cells for CAP to downregulate systemic inflammatory responses [18]. To elucidate the role of signals of vagal circuits in

regulating local (lung) inflammatory responses, we postulated a pulmonary parasympathetic inflammatory reflex [30, 31] in which $\alpha 7$ nAChR-expressing CD11b⁺ and Gr1⁺ cells are efferent arms of this reflex. Activation of $\alpha 7$ nAChR with ACh (neurotransmitter of vagal circuits) in CD11b⁺ cells could dampen *E. coli* and LPS-induced inflammatory responses [30, 31]. Disruption of vagal circuits inactivated $\alpha 7$ nAChR in CD11b⁺ cells and reduced *E. coli* and LPS-induced inflammatory responses.

Our data showed that more CD11b⁺ granulocytes were discharged from spleen and recruited to the lung in *E. coli*-infected *Chrna7*^{-/-} mice. The *E. coli*-infected *Akt1*^{-/-} mice shared the similar phenotype as *Chrna7*^{-/-} mice, suggesting that AKT1 has a role in regulating flux and function of $\alpha 7$ nAChR-expressing CD11b⁺ cells. CD11b is a negative regulator for TLR4 signaling and CD11b-deficient mice were susceptible to bacterial infection [41]. There were more CD11b⁺ cells presented in *E. coli*-infected *Chrna7*^{-/-} or *Akt1*^{-/-} lung, but inflammation was worsened, suggesting that CD11b is not able to exert inhibitory effect on inflammation without function of $\alpha 7$ nAChR and AKT1.

On the basis of the results of these experiments, did the spleen alone account for the accumulation of CD11b⁺ cells in the lungs? Considering that mobilization of bone marrow proinflammatory cells is an important pathological process in response to lung infection [46], we had to clarify whether bone marrow was a source of inflammatory cells under *E. coli*-infected vagotomized and *Chrna7*^{-/-}*Itgam*^{-/-} conditions. By flow cytometry, we found that changes of monocytes and neutrophils in the bone marrow were not in accordance with changes of accumulated lung

Figure 6 Deficiency of $\alpha 7$ nAChR enhances release of CD11b⁺ cells from spleen and recruitment of these cells towards the injured lungs by reducing phosphorylation of AKT1^{Ser473+}. (a–f) Deletion of *Chrna7* reduces serine phosphorylation of AKT1 in the spleen and lung cells during *E. coli* pneumonia. Wildtype and *Chrna7*-deleted mice were IT challenged with *E. coli* (2.5×10^6 cfu). The mice were killed at 24 h after *E. coli* challenge. The spleen (a) and lung (d) cells were isolated and labeled with PE-anti-p-AKT1^{Ser473} antibody after permeabilization. The whole-cell population was gated (b, e). p-AKT1^{Ser473+} cells were analyzed (c, f). The percentage of p-AKT1^{Ser473+} cells was presented. $N = 4$ in each group, $*P < 0.05$, Student's *t*-test. Data are presented as mean \pm s.d. (g, h) Deletion of *Chrna7* affects lung neutrophils and *E. coli* colonies during lung infection. Wildtype and *Chrna7*-deleted mice were IT challenged with *E. coli* (2.5×10^6 cfu). The mice were killed at 24 h after *E. coli* challenge. Lungs cells were counted by Wright's staining (g). Serial dilution of the supernatant of homogenized lung and bacterial culture was used to detect *E. coli* colonies (h). $N = 4$ in each group, $*P < 0.05$, Student's *t*-test. Data are presented as mean \pm s.d. (i–k) Depletion of *Chrna7* reduces splenic CD11b⁺ cells during *E. coli* pneumonia. The wildtype, *Chrna7*^{-/-}, *Akt1*^{-/-} and *Itgam*^{-/-} mice were, respectively, challenged with *E. coli* (2.5×10^6 cfu) intratracheally. The mice were killed at 24 h after *E. coli* challenge. The spleen cells were isolated and labeled with PE-anti-CD11b antibody. The granular cells were gated (i) in each group (j). The percentage of CD11b⁺ cells was presented (k). $N = 3–4$ in each group, $*P < 0.05$. Data are presented as mean \pm s.d. (l–n) Depletion of *Chrna7* increases BAL CCR2⁺CD11b⁺ cells during *E. coli* pneumonia. The wildtype and *Chrna7*^{-/-} mice were respectively challenged with *E. coli* (2.5×10^6 cfu) intratracheally. The mice were killed at 24 h after *E. coli* challenge. The BAL cells were isolated and labeled with FITC-anti-CCR2 and PE-anti-CD11b antibodies. The larger granular and smaller granular cells were separately gated (l, m). The percentage of CCR2⁺CD11b⁺ cells was calculated (n). $N = 3–4$ in each group, $*P < 0.05$, student's *t*-test. Data are presented as mean \pm s.d.

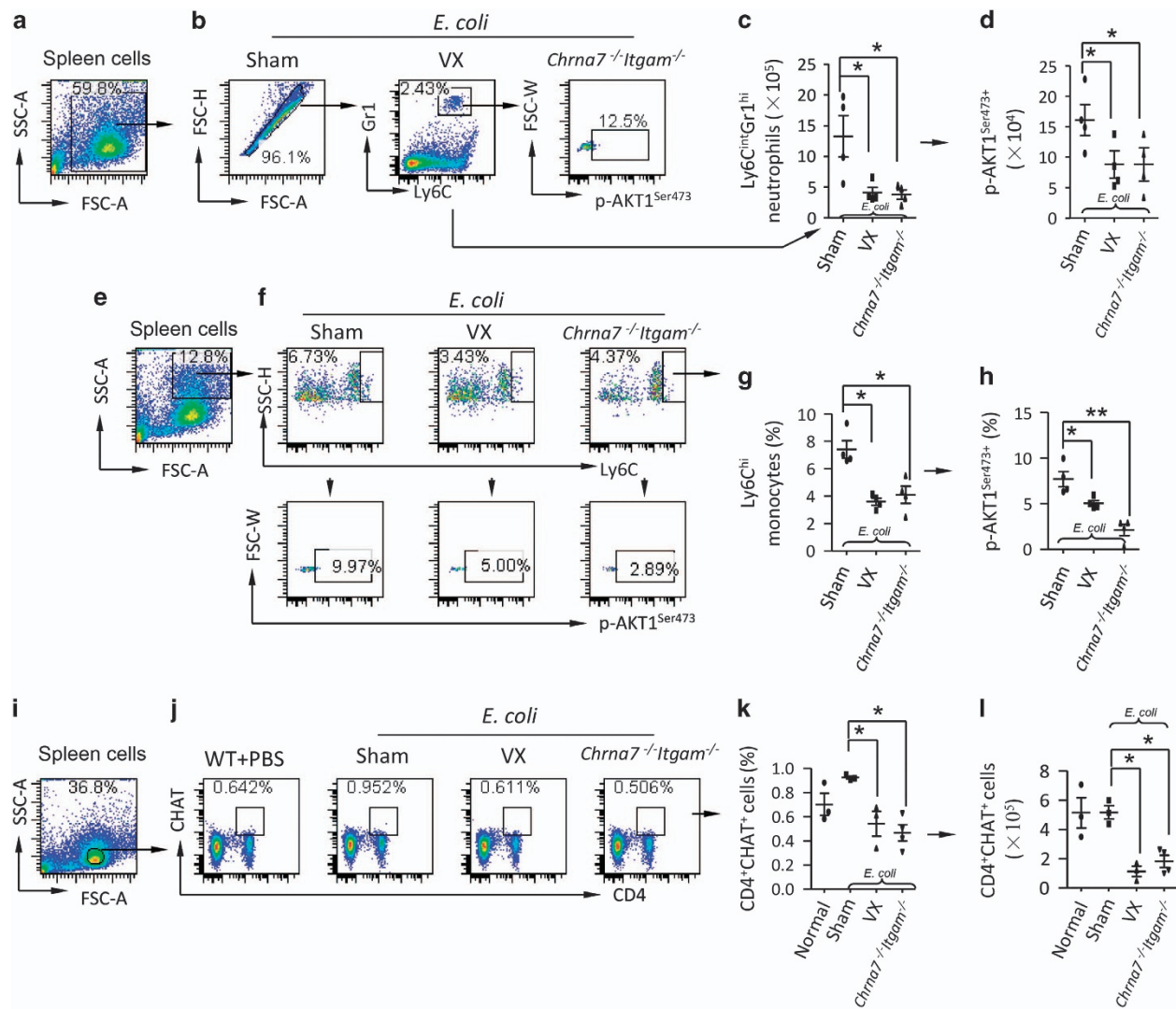


Figure 7 Vagotomy and double deletion of *Chrna7* and *Itgam* reduce p-AKT1^{Ser473+} neutrophils and monocytes and ACh-producing CD4⁺CHAT⁺ cells during *E. coli* pneumonia. (a–d) Flow cytometry analysis of AKT1^{Ser473} phosphorylation in splenic neutrophils. The sham, vagotomized and *Chrna7*^{-/-}*Itgam*^{-/-} mice were IT challenged with *E. coli* (2.5×10^6 cfu). The mice were killed at 24 h after *E. coli* challenge. Spleen cells were collected and labeled with fluorescent antibodies. (a) Whole-cell population was gated. (b) Ly6C^{int}Gr1^{hi} neutrophils were grouped, then subgated p-AKT1^{Ser473+} cells. (c) Number of splenic Ly6C^{int}Gr1^{hi} neutrophils. (d) Number of p-AKT1^{Ser473+} cells in Ly6C^{int}Gr1^{hi} gate. $N = 4$ in each group, $*P < 0.05$. Data are presented as mean \pm s.d. (e–h) Flow cytometry analysis of AKT1^{Ser473} phosphorylation in splenic monocytes. Using the same experimental setting as (a–d), granular cells were gated (e). Ly6C^{hi} monocytes were grouped, then subgrouped for p-AKT1^{Ser473+} monocytes (f). (g) Percentage of BAL monocytes. (h) Percentage of p-AKT1^{Ser473+} monocytes was presented. $N = 4$ in each group, $*P < 0.05$, $**P < 0.01$. (i–l) Flow cytometry analysis of splenic ACh-producing CD4⁺CHAT⁺ cells during *E. coli* pneumonia. Using the same experimental setting as (a–d), the four groups of spleen cells were subjected to flow cytometric analysis. (i) Lymphocyte population was gated. (j) CD4⁺CHAT⁺ cells were subgated. (k) Percentage of splenic CD4⁺CHAT⁺ cells. (l) Number of CD4⁺CHAT⁺ cells was calculated by multiplying the percentage with total spleen cell counts. $N = 4$ in each group, $*P < 0.05$. Data are presented as mean \pm s.d.

proinflammatory cells. Furthermore, peritoneal macrophages are resident cells and these cells do not migrate to the lung during lung infection and inflammation. Therefore, our findings strongly suggest that lung inflammatory cells are most likely recruited from

the spleen under *E. coli*-infected vagotomized and *Chrna7*^{-/-}*Itgam*^{-/-} conditions.

Another important question is why neutrophils and monocytes accumulated in the vagotomized and *Chrna7*^{-/-}*Itgam*^{-/-} lungs but did not reduce bacterial

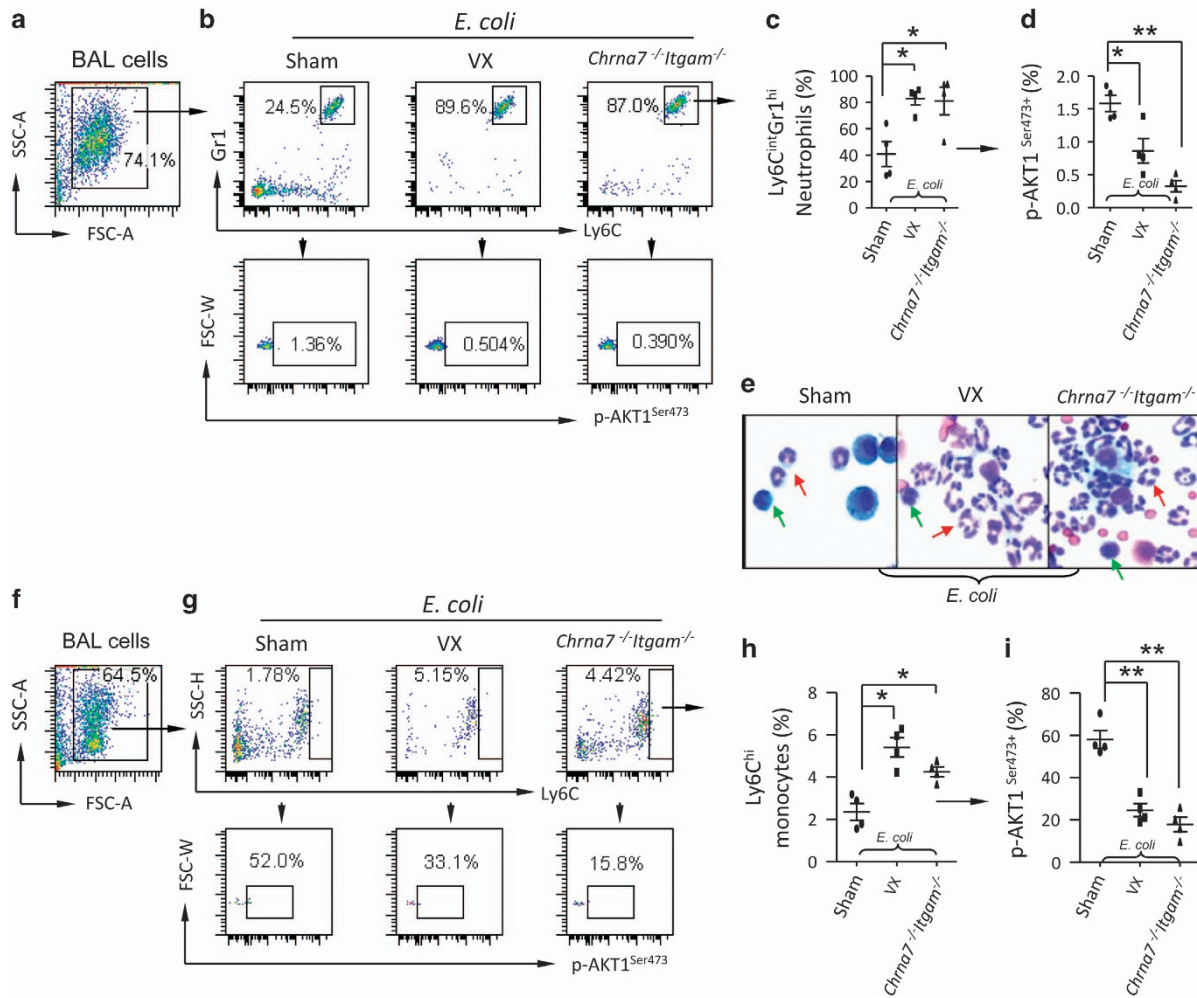


Figure 8 Vagotomy and double deletion of *Chrna7* and *Ilgam* reduce AKT1^{Ser473} phosphorylation in BAL neutrophils and monocytes during *E. coli* pneumonia. The sham, vagotomized and *Chrna7*^{-/-}*Ilgam*^{-/-} mice were IT challenged with *E. coli* (2.5×10^6 cfu). The mice were killed at 24 h after *E. coli* challenge. BAL cells were collected and labeled with Fluorescent antibodies. (a–d) Flow cytometry analysis of AKT1^{Ser473} phosphorylation in BAL neutrophils. (a) Whole-cell population was gated. (b) Ly6C^{int}Gr1^{hi} neutrophils were estimated in each group. (c) Percentage of BAL neutrophils. (d) Percentage of p-AKT1^{Ser473+} neutrophils was calculated. *N* = 4 in each group, **P* < 0.05, ***P* < 0.01. Data are presented as mean ± s.d. (e) Representative micrograph of Hema3 staining of BAL cells collected from *E. coli*-infected sham, vagotomized and *Chrna7*^{-/-}*Ilgam*^{-/-} mice. Red arrows indicate neutrophils; green arrows denote monocytes. (f–i) Flow cytometry analysis of AKT1^{Ser473} phosphorylation in BAL monocytes. (f) Whole-cell population was gated. (g) Ly6C^{hi} monocytes were subgated for p-AKT1^{Ser473+} monocytes. (h). Percentage of BAL monocytes. (i) Percentage of p-AKT1^{Ser473+} monocytes was presented. *N* = 4 in each group, **P* < 0.05, ***P* < 0.01. Data are presented as mean ± s.d.

infection. The possible explanation is that acetylcholine or $\alpha 7$ nAChR agonist could modify their anti-bacterial properties. Sitapara *et al.* [47] reported that activation of $\alpha 7$ nAChR by GTS-21 is effective in improving bacterial clearance and decreasing acute lung injury. GTS-21 can improve the phagocytic ability of hyperoxic macrophages. It was found that cholinergic stimulation enhanced the antimicrobial immune response leading to effective control of bacterial proliferation and improved survival [48].

ChAT-expressing T cells were found to control the host antimicrobial peptide secretion, microbial growth and expansion [49]. Serhan’s group reported that *E. coli* phagocytosis was impaired in peritoneal exudate Ly6G⁺ CD11b⁺ neutrophils in right cervical vagotomized mice [50]. They found that peritoneal acetylcholine levels were significantly reduced d1, 3 and 7 post right cervical vagotomy [50]. Right rather than left vagus nerve regulates host responses to bacterial infection [50]. Dissection of the right vagus decreased peritoneal group

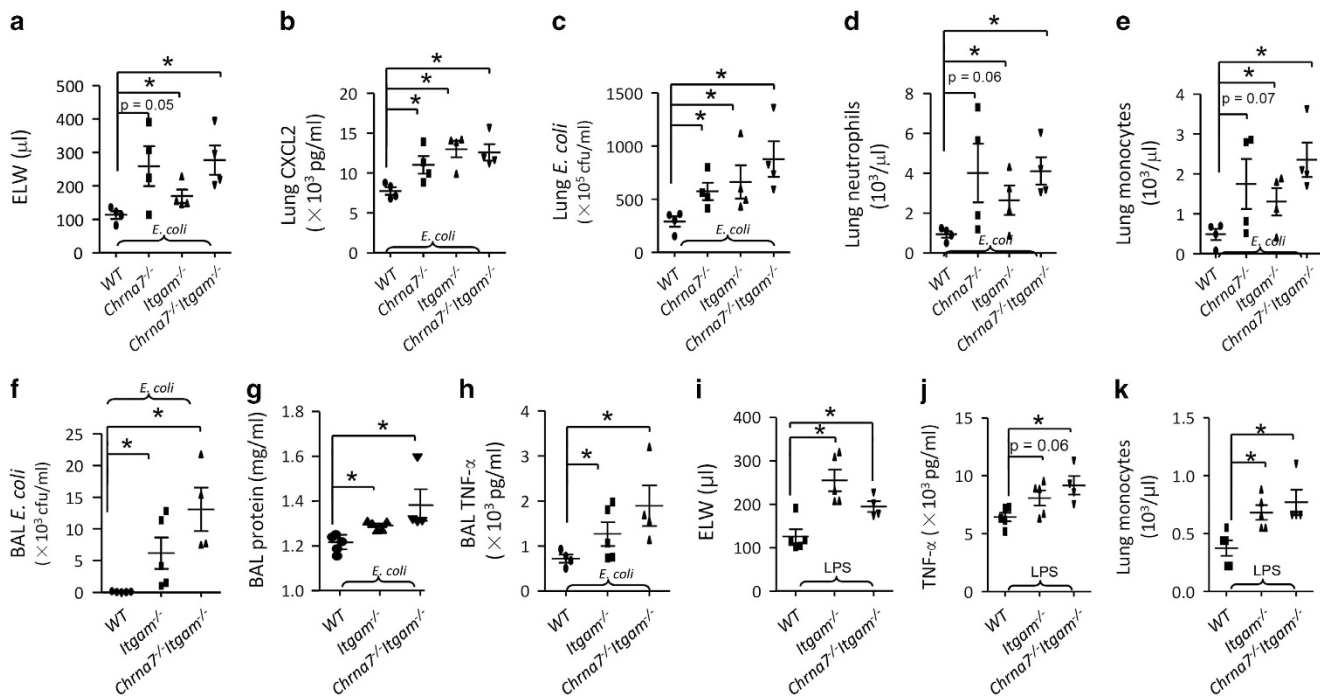


Figure 9 Deletion of *Itgam* or/and *Chrna7* worsens *E. coli* and LPS-induced ALI. Double deletion of *Chrna7* and *Itgam* aggravates *E. coli*-induced ALI (a–e). The wildtype, *Chrna7*^{-/-}, *Itgam*^{-/-} and *Chrna7*^{-/-}*Itgam*^{-/-} mice were, respectively, challenged with *E. coli* (2.5×10^6 cfu) intratracheally. The mice were killed at 24 h after *E. coli* challenge. ELW (a), CXCL2 levels (b) in the supernatant of lung homogenate, lung *E. coli* colonies (c), lung neutrophils (d) and lung monocytes (e) were measured. $N = 4$ in each group, $*P < 0.05$, one-way ANOVA with Bonferroni *post hoc* test. Data are presented as mean \pm s.d. Double deletion of *Chrna7* and *Itgam* increases BAL inflammatory parameters in *E. coli*-induced ALI (f–h). The wildtype, *Itgam*^{-/-} and *Chrna7*^{-/-}*Itgam*^{-/-} mice were, respectively, challenged with *E. coli* (2.5×10^6 cfu) intratracheally. The mice were killed at 24 h after *E. coli* challenge. BAL was collected to measure BAL *E. coli* colonies (f), BAL protein (g) and BAL TNF- α (h). $N = 4$ in each group, $*P < 0.05$, one-way ANOVA with Bonferroni *post hoc* test. Data are presented as mean \pm s.d. (i–k) Double deletion of *Chrna7* and *Itgam* exacerbates LPS-induced ALI. The wildtype, *Itgam*^{-/-} and *Chrna7*^{-/-}*Itgam*^{-/-} mice were, respectively, challenged with LPS (5 mg kg^{-1}) intratracheally. The mice were killed at 24 h after LPS challenge. ELW (i), TNF- α level (j) in the supernatant of lung homogenate and lung monocytes (k) were analyzed. $N = 5$ in each group, $*P < 0.05$, one-way ANOVA with Bonferroni *post hoc* test. Data are presented as mean \pm s.d.

3 innate lymphoid cell (ILC3) numbers and altered peritoneal macrophage responses to bacteria infection. Stimulation of acetylcholine in ILC3s could enhance yield of immunosolvent PCTR1, which protected bacterial infection [50]. ILC3 is the major source of IL-22, and the later is a protective mediator of mucosa immunity [51, 52]. In this study, lung *Il22* mRNA was reduced and *Cxcl2* mRNA was increased in *E. coli*-challenged vagotomized and *Chrna7*^{-/-}*Itgam*^{-/-} mice compared to the control. The findings suggested that vagotomy and deficiency of $\alpha 7$ nAChR and CD11b compromise anti-bacterial capacity and promote proinflammatory cytokine production.

A third issue is how AKT1 regulates migration of proinflammatory cells. It has been reported that AKT1-deficient neutrophils exhibit an enhanced migration and production of proinflammatory

cytokines [43]. AKT1 has a negative role in regulating migration of neutrophils and development of acute inflammation [53–55]. In this study, the p-AKT1^{Ser473} levels were markedly decreased in the isolated neutrophils from LPS-challenged vagotomized mice. Activation of $\alpha 7$ nAChR promoted phosphorylation of AKT1^{Ser473} and inhibited CXCL2 production. Inhibition of phosphorylation of AKT1^{Ser473} enhanced CXCL2 production in neutrophils. Vagotomy markedly decreased phosphorylation of AKT1^{Ser473} in splenic and BAL $\alpha 7$ nAChR⁺CD11b⁺ cells, or Ly6C^{int}Gr1^{hi} neutrophils and Ly6C^{hi} monocytes, facilitated alveolar recruitment of inflammatory cells, and deteriorated lung inflammation. In addition, phosphorylation of Bax Ser184 by AKT regulates its activity and apoptosis in neutrophils [56]. Initiation of the apoptotic process inhibits the ability of neutrophils to move, degranulate,

and produce superoxide [57]. AKT1 might be essential to induce NADPH-dependent NETosis and to switch the neutrophil death to apoptosis [58]. Inflammatory mediators could inhibit apoptosis of neutrophils and prolong neutrophil functional longevity [57]. Therefore, we speculate that AKT1 might regulate migration of neutrophils via impacting on apoptosis, which is worthy of further investigation in the future.

Another issue is to determine the fate of CD4⁺CHAT⁺ lymphocytes in the spleen. Spleen CD4⁺CHAT⁺ lymphocytes synthesize acetylcholine and render anti-inflammatory activity to splenic Ly6C^{int}Gr1^{hi} neutrophils and Ly6C^{hi} monocytes via phosphorylation of AKT1. Vagotomy and double deletion of *Chrna7* and *Itgam* reduced spleen CD4⁺CHAT⁺ lymphocytes. The percentage of CD4⁺ T cells was reduced, suggesting that CD4⁺ T cells might egress from vagotomized spleens or undergo apoptotic. However, this finding is not consistent with the previous report that vagotomy facilitated proliferation of CD4⁺ T cells [59]. The spleen receives innervation of both sympathetic and parasympathetic nerves [60, 61]. Activation of sympathetic β 2-adrenergic receptor promotes CHAT expression in the spleen. We found that CHAT expression was reduced in *Chrna7*^{-/-}*Itgam*^{-/-} spleens. This finding suggests that α 7 nAChR or/and CD11 also regulate CHAT expression as a feedback.

The anti-inflammatory role of CAP in the spleen was confirmed by splenectomy, [18, 23, 24] as splenectomy could inactivate CAP during lethal endotoxemia and polymicrobial sepsis [23]. However, some studies have demonstrated that splenectomy protected against sepsis lethality and reduced serum HMGB1 levels [62], and splenectomy was detrimental to the immune response to lung infection [63]. Splenectomy causes immunologic impairment and increases susceptibility to infection [64–66]. Therefore, splenectomy might confound the findings of *E. coli* lung infection.

We aimed to observe acute effect of vagotomy on lung infection and inflammation, so we chose challenging the mice immediately after vagotomy. However, a study suggested that surgical vagotomy reduced plasma TNF- α production probably because of nerve damage-triggered ACh release [67], but blood ACh levels were not measured in that study. In this study, α 7 nAChR agonist could reverse LPS and *E. coli*-induced lung proinflammatory responses deteriorated by vagotomy, and this result does not support that vagotomy triggers release of ACh. Pulmonary neurectomy might be an alternative way to test specificity of vagal denervation on lung recruitment of

α 7 nAChR⁺CD11b⁺ cells and development of inflammation. However, the pulmonary branches of vagus nerve are joined by filaments from sympathetic nerve; it is impractical to selectively disrupt lung vagal innervation.

In summary, during *E. coli* and LPS-induced ALI, splenic CD4⁺CHAT⁺ cells can synthesize ACh, which activates α 7 nAChR in CD11b⁺ cells (monocytes and neutrophils) to elicit phosphorylation of AKT1, stabilizes α 7 nAChR⁺CD11b⁺ cells in the spleen and decreases recruitment of α 7 nAChR⁺CD11b⁺ cells towards the injured lung. In addition, vagal efferent nerve endings innervate distal lung parenchyma or alveoli where ACh is released upon infection or LPS stimulation. Activation of α 7 nAChR by ACh in the recruited CD11b⁺ cells could mitigate production of proinflammatory cytokines and bacterial growth and therefore attenuate lung inflammation and infection. Disruption of vagal circuits reduces synthesis of ACh in CD4⁺CHAT⁺ cells and impairs phosphorylation of AKT1 of α 7 nAChR⁺CD11b⁺ cells in the spleen. This event facilitates splenic egress and lung recruitment of α 7 nAChR⁺CD11b⁺ cells. Disruption of intact vagal circuits or lack of sufficient ACh impairs phosphorylation of AKT1 in the recruited α 7 nAChR⁺CD11b⁺ cells. The proinflammatory responses in these cells could not be efficiently attenuated. Similar to vagotomy, double deletion of *Chrna7* and *Itgam* reduces splenic CD4⁺CHAT⁺ cells and phosphorylation of AKT1 in neutrophils and monocytes, and promote recruitment of these cells to the lung where lung proinflammatory responses are propagated (Supplementary Figure S13). Thus, signals of vagal circuits engaging with phosphorylation of AKT1 in α 7 nAChR⁺CD11b⁺ cells attenuate *E. coli* and LPS-induced acute lung inflammatory responses.

Materials and Methods

Animals

Chrna7^{-/-}, B6.129S7-*Chrna7*^{tm1Bay}/J; *Akt1*^{-/-}, B6.129P2-*Akt1*^{tm1Mbb}/J; *Itgam*^{-/-}, B6.129S4-*Itgam*^{tm1Myd}/J; *Tlr4*^{-/-}, B6.10ScN-*Tlr4*^{lps-del}/*JthJ* and wildtype mice (C57BL/6) were purchased from the Jackson Laboratory (Bar Harbor, ME, USA) and the Model Animal Research Center of Nanjing University (Nanjing, China). LysM-EGFP was from E. Robey (UC, Berkeley, CA, USA) [45]. The mice were housed with 12 h dark/light cycles and with free access to food and water. Anesthesia was induced with an intraperitoneal (ip) injection of a mixture of xylazine (10 mg kg⁻¹) and ketamine (90 mg kg⁻¹) or pentobarbital sodium (50 mg kg⁻¹). The Committees on Animal Research of the Institut Pasteur of Shanghai, Chinese Academy of Sciences approved the animal studies.

Mouse animal models

Procedures to establish LPS-induced ALI and *E. coli* pneumonia have been published in our previous studies [28, 29]. There was no death in both control and treated groups if receiving an IT *E. coli* (2.5×10^6 cfu) at 24 h [29].

Unilateral vagotomy

Right or sham cervical vagotomy was performed with the animals under anesthesia. The procedure involved a longitudinal midline incision in the ventral region of the neck. Using blunt dissection, the overlying muscles and fascia were separated until the right vagus and carotid artery were visible. The vagus was carefully stripped away from carotid artery and lightly cut off in the vagotomy group. The vagus was kept intact in sham group. The wound was closed and sutured. The respiration rhythm was not affected by unilateral vagotomy. It is reported that right nerve controls cardiac function and this side is not chosen for vagus nerve stimulation [68]. In our study, comparing sham to vagotomy mice receiving an IT of saline, there no any difference in BAL cytokines and inflammatory cell profiles within 24 h. No mice died of heart failure after right side of vagotomy.

Reagents

DMAB-anabaseine dihydrochloride and PHA568487 were from Tocris Biosciences (Minneapolis, MN, USA); (-)-Nicotine hemisulfate salt and LPS *E. coli* 0111:B4 were from Sigma (St Louis, MO, USA). Anti-mouse Ly6C APC, anti-mouse CD11b PE, anti-mouse Gr1 FITC and PE, anti-mouse CD4 FITC and PE, anti-mouse CD16/CD32 antibodies and IgG isotype controls were from eBioscience (San Diego, CA, USA). For immunofluorescence, anti-mouse CD11b and Gr1 antibodies were from BD Biosciences (San Jose, CA, USA). Phospho-Akt1 (Ser473) (D7F10) XP rabbit mAb (Akt1 Specific) and PathScan Phospho-Akt1 (Ser473) Sandwich ELISA Kit were from Cell Signaling (Danvers, MA, USA); AChR α 7 antibody (H-302) was from Santa Cruz Biotechnology (Santa Cruz, CA, USA). Mouse CCR2 APC-conjugated antibody and mouse CXCL2 and TNF- α ELISA Kit were from R&D Systems (Minneapolis, MN, USA). Anti-Choline acetyltransferase antibody was from Abcam (Cambridge, MA, USA). *E. coli* K1 (serotype) strain, isolated from patients with biliary infection, was kindly provided by Dr Thomas Martin (University of Washington, USA) [69].

Measurement of ELW

The detailed procedures were described previously [28]. Briefly, homogenate and supernatant of lung, and blood were weighed and then desiccated in an oven (60 °C for 24 h). ELW was calculated by standard formula:

$$\text{ELW} = \left[\left(\frac{Q_{w,\text{exp}}}{Q_{d,\text{exp}}} \times Q_{d,\text{exp}} \right) - \left(\frac{Q_{w,\text{control}}}{Q_{d,\text{control}}} \times Q_{d,\text{control}} \right) \right] \times 1000 (\mu\text{l})$$

where $Q_{w,\text{exp}}$ equals water volume of the lung in the experimental group; $Q_{d,\text{exp}}$ equals dry weight of lung in the experimental group. The controls were the normal mice with the same age as the experimental group.

Immunofluorescence and determination of lung myeloperoxidase activity

Briefly, we performed Immunofluorescence referring to the previous study [29]. To measure lung myeloperoxidase (MPO) activity, the supernatants of lung homogenate were mixed with *o*-dianisidine HCl (Sigma-Aldrich) and H₂O₂ to measure optical density by a spectrophotometer at 405 nm using our established method [29].

Bronchoalveolar lavage, protein levels and leukocyte counts and differentiation

The detailed procedures were described previously [28, 29]. The mice were intubated with a 24-gauge cannula after their tracheas were surgically isolated. The lungs were flushed with 1 ml PBS back and forth for 3 times. Protein concentration in the BAL was determined by a Bio-Rad protein assay (Bio-Rad Laboratories, Hercules, CA, USA). BAL cell smear was made using cytospin (Shandon, Pittsburgh, PA, USA). The slides were visualized using Hema3 staining (Fisher Scientific, Middletown, VA, USA). Neutrophils and monocytes were identified by a certified laboratory technologist in a blinded fashion. BAL cells were also used for flow cytometry analysis after lysing erythrocytes.

Complete blood count

Using a multispecies hematology instrument (Hemavet 950FS; Drew Scientific, Dallas, TX, USA), we measured blood neutrophils, monocytes, hematocrit and other parameters [40].

Preparation of lung cells, spleen and blood cells

Harvested lungs were inflated with 3 ml of a mixture of collagenase (150 U ml⁻¹) and DNaseI (10 μ g ml⁻¹) in RPMI-1640 containing 5% FBS and 20 mM HEPES. Lungs were chopped in the 3 ml enzyme mix and incubated for 35 min at 37 °C. Overall, 10 mM EDTA was added and any remaining pieces were further dispersed by 12 passages through a 21-G needle. Suspensions were passed through a 100 μ m nylon mesh and cells were washed multiple times in RPMI-1640 with 5% FBS, 20 mM HEPES. RBC lysis was performed on cell preparations for cellular analysis by flow cytometry. For preparing single cells, spleens were removed and grounded in a 70 μ m cell strainer. Erythrocytes were lysed [11]. For preparing blood leukocytes, we utilized BD Pharm Lyse-Lysing Buffer (BD Biosciences) to lyse erythrocytes.

Flow cytometric analysis

After unspecific staining was minimized through pre-incubation for 15 min with anti-mouse CD16/32 antibodies, lung, spleen, blood or BAL cells were labeled with primary or isotype antibodies. Isotype antibody and unstained controls were used to demonstrate specificity of staining and to establish the criteria for flow cytometry populations (for simplicity, data are not presented regarding these controls). The data fluorescent cells were analyzed after excluding debris and aggregates with LSRFortessa (BD Biosciences). Data were analyzed by *Flowjo* 7.6 software (Tree Star, Ashland, OR, USA).

Measurements of cytokine levels by ELISA

TNF- α , CXCL2, and phospho-Akt1 (Ser473) levels in the biofluid were measured by ELISA kits according to the manufacturers' instructions.

Statistical analysis

Statistics analysis was performed using GraphPad Prism software (GraphPad, San Diego, CA, USA). For multiple comparisons, we chose one-way ANOVA with Bonferroni *post hoc* test. For comparing two groups, we approached a Student's *t*-test. For repeated measures, we used two-way ANOVA. We examined difference of survival by a log-rank test. Significance level was set at $P < 0.05$. The results are shown as mean \pm s.d.

Conflict of Interest

The authors declare no conflict of interest.

Acknowledgements

Our research is supported by the Major Research Plan of 81470269, NSFC 91542105 and NSFC 81270139 (XS); the 100 Talents Project of the CAS 2A2013311211004 (XS); The Knowledge Innovation Program of the CAS 24P201200201 (XS); The STS Plan of CAS KFJ-EW-STS-098 (XS); and The Shanghai Key Grant 12JC1408900 (XS); NHLBI Grants HL-51854 and NIAID AI53194 (to MAM); and a Parker B. Francis Award (to XS). We appreciate Yiyi Jiang for breeding animals.

Author contributions

XS and MAM designed the research and provided financial support and study material; XS, CZ, XY, EMS, YH and LL performed experiments and collected data; XS analyzed data; XS and MAM wrote the manuscript; XS approved of final manuscript.

References

- 1 Ware LB, Matthay MA. The acute respiratory distress syndrome. *N Engl J Med* 2000; **342**: 1334–1349.
- 2 Wiener-Kronish JP, Gropper MA, Matthay MA. The adult respiratory distress syndrome: definition and prognosis, pathogenesis and treatment. *Br J Anaesth* 1990; **65**: 107–129.
- 3 Pittet JF, Mackersie RC, Martin TR, Matthay MA. Biological markers of acute lung injury: prognostic and pathogenetic significance. *Am J Respir Crit Care Med* 1997; **155**: 1187–1205.
- 4 Kaslovsky RA, Parker K, Siflinger-Birnboim A, Malik AB. Increased endothelial permeability after neutrophil activation occurs by a diffusion-dependent mechanism. *Microvasc Res* 1995; **49**: 227–232.
- 5 Gardinali M, Borrelli E, Chiara O *et al.* Inhibition of CD11-CD18 complex prevents acute lung injury and reduces mortality after peritonitis in rabbits. *Am J Respir Crit Care Med* 2000; **161**: 1022–1029.
- 6 Zhou MY, Lo SK, Bergenfeldt M *et al.* *In vivo* expression of neutrophil inhibitory factor via gene transfer prevents lipopolysaccharide-induced lung neutrophil infiltration and injury by a beta2 integrin-dependent mechanism. *J Clin Invest* 1998; **101**: 2427–2437.
- 7 Su X. Leading neutrophils to the alveoli: who is the guider? *Am J Respir Crit Care Med* 2012; **186**: 472–473.
- 8 Dhaliwal K, Scholefield E, Ferenbach D *et al.* Monocytes control second-phase neutrophil emigration in established lipopolysaccharide-induced murine lung injury. *Am J Respir Crit Care Med* 2012; **186**: 514–524.
- 9 Tracey KJ. The inflammatory reflex. *Nature* 2002; **420**: 853–859.
- 10 Andersson J. The inflammatory reflex—introduction. *J Intern Med* 2005; **257**: 122–125.
- 11 Gabanyi I, Muller PA, Feighery L, Oliveira TY, Costa-Pinto FA, Mucida D. Neuro-immune interactions drive tissue programming in intestinal macrophages. *Cell* 2016; **164**: 378–391.
- 12 Andersson U, Tracey KJ. Neural reflexes in inflammation and immunity. *J Exp Med* 2012; **209**: 1057–1068.
- 13 Ogbonnaya S, Kaliaperumal C. Vagal nerve stimulator: evolving trends. *J Nat Sci Biol Med* 2013; **4**: 8–13.
- 14 Pavlov VA, Tracey KJ. Neural regulators of innate immune responses and inflammation. *Cell Mol Life Sci* 2004; **61**: 2322–2331.
- 15 Gallowitsch-Puerta M, Pavlov VA. Neuro-immune interactions via the cholinergic anti-inflammatory pathway. *Life Sci* 2007; **80**: 2325–2329.
- 16 Tracey KJ. Reflex control of immunity. *Nat Rev Immunol* 2009; **9**: 418–428.
- 17 Tracey KJ. Reflexes in Immunity. *Cell* 2016; **164**: 343–344.
- 18 Rosas-Ballina M, Olofsson PS, Ochani M *et al.* Acetylcholine-synthesizing T cells relay neural signals in a vagus nerve circuit. *Science* 2011; **334**: 98–101.
- 19 Andersson U, Tracey KJ. Reflex principles of immunological homeostasis. *Ann Rev Immunol* 2012; **30**: 313–335.
- 20 Rosas-Ballina M, Tracey KJ. The neurology of the immune system: neural reflexes regulate immunity. *Neuron* 2009; **64**: 28–32.
- 21 Wang H, Liao H, Ochani M *et al.* Cholinergic agonists inhibit HMGB1 release and improve survival in experimental sepsis. *Nat Med* 2004; **10**: 1216–1221.
- 22 Wang H, Yu M, Ochani M *et al.* Nicotinic acetylcholine receptor alpha7 subunit is an essential regulator of inflammation. *Nature* 2003; **421**: 384–388.
- 23 Huston JM, Ochani M, Rosas-Ballina M *et al.* Splenectomy inactivates the cholinergic antiinflammatory pathway during lethal endotoxemia and polymicrobial sepsis. *J Exp Med* 2006; **203**: 1623–1628.
- 24 Rosas-Ballina M, Ochani M, Parrish WR *et al.* Splenic nerve is required for cholinergic antiinflammatory pathway control of TNF in endotoxemia. *Proc Natl Acad Sci USA* 2008; **105**: 11008–11013.

- 25 Fox B, Bull TB, Guz A. Innervation of alveolar walls in the human lung: an electron microscopic study. *J Anat* 1980; **131**: 683–692.
- 26 Hertweck MS, Hung KS. Ultrastructural evidence for the innervation of human pulmonary alveoli. *Experientia* 1980; **36**: 112–113.
- 27 Livermore S, Zhou Y, Pan J, Yeger H, Nurse CA, Cutz E. Pulmonary neuroepithelial bodies are polymodal airway sensors: evidence for CO₂/H⁺ sensing. *Am J Physiol Lung Cell Mol Physiol* 2015; **308**: L807–L815.
- 28 Su X, Lee JW, Matthay ZA *et al.* Activation of the alpha7 nAChR reduces acid-induced acute lung injury in mice and rats. *Am J Respir Cell Mol Biol* 2007; **37**: 186–192.
- 29 Su X, Matthay MA, Malik AB. Requisite role of the cholinergic alpha7 nicotinic acetylcholine receptor pathway in suppressing Gram-negative sepsis-induced acute lung inflammatory injury. *J Immunol* 2010; **184**: 401–410.
- 30 Yang X, Zhao C, Gao Z, Su X. A novel regulator of lung inflammation and immunity: pulmonary parasympathetic inflammatory reflex. *QJM* 2014; **107**: 789–792.
- 31 Wu H, Li L, Su X. Vagus nerve through alpha7 nAChR modulates lung infection and inflammation: models, cells, and signals. *Biomed Res Int* 2014; **2014**: 283525.
- 32 Huston JM, Rosas-Ballina M, Xue X *et al.* Cholinergic neural signals to the spleen down-regulate leukocyte trafficking via CD11b. *J Immunol* 2009; **183**: 552–559.
- 33 Davis HM, Carpenter DC, Stahl JM, Zhang W, Hynicka WP, Griswold DE. Human granulocyte CD11b expression as a pharmacodynamic biomarker of inflammation. *J Immunol Methods* 2000; **240**: 125–132.
- 34 Zhou X, Gao XP, Fan J *et al.* LPS activation of Toll-like receptor 4 signals CD11b/CD18 expression in neutrophils. *Am J Physiol Lung Cell Mol Physiol* 2005; **288**: L655–L662.
- 35 Fan ST, Edgington TS. Integrin regulation of leukocyte inflammatory functions. CD11b/CD18 enhancement of the tumor necrosis factor-alpha responses of monocytes. *J Immunol* 1993; **150**: 2972–2980.
- 36 Powner DJ, Pettitt TR, Anderson R, Nash GB, Wakelam MJ. Stable adhesion and migration of human neutrophils requires phospholipase D-mediated activation of the integrin CD11b/CD18. *Mol Immunol* 2007; **44**: 3211–3221.
- 37 Zen K, Guo YL, Li LM, Bian Z, Zhang CY, Liu Y. Cleavage of the CD11b extracellular domain by the leukocyte serprocidins is critical for neutrophil detachment during chemotaxis. *Blood* 2011; **117**: 4885–4894.
- 38 Overbeek SA, Kleinjan M, Henricks PA *et al.* Chemo-attractant N-acetyl proline-glycine-proline induces CD11b/CD18-dependent neutrophil adhesion. *Biochim Biophys Acta* 2013; **1830**: 2188–2193.
- 39 Zhang X, Bajic G, Andersen GR, Christiansen SH, Vorup-Jensen T. The cationic peptide LL-37 binds Mac-1 (CD11b/CD18) with a low dissociation rate and promotes phagocytosis. *Biochim Biophys Acta* 2016; **1864**: 471–478.
- 40 Wan M, van der Does AM, Tang X, Lindbom L, Agerberth B, Haeggstrom JZ. Antimicrobial peptide LL-37 promotes bacterial phagocytosis by human macrophages. *J Leukoc Biol* 2014; **95**: 971–981.
- 41 Han C, Jin J, Xu S, Liu H, Li N, Cao X. Integrin CD11b negatively regulates TLR-triggered inflammatory responses by activating Syk and promoting degradation of MyD88 and TRIF via Cbl-b. *Nat Immunol* 2010; **11**: 734–742.
- 42 Dajas-Bailador F, Wonnacott S. Nicotinic acetylcholine receptors and the regulation of neuronal signalling. *Trends Pharmacol Sci* 2004; **25**: 317–324.
- 43 Liu G, Bi Y, Wang R *et al.* Kinase AKT1 negatively controls neutrophil recruitment and function in mice. *J Immunol* 2013; **191**: 2680–2690.
- 44 Swirski FK, Nahrendorf M, Etzrodt M *et al.* Identification of splenic reservoir monocytes and their deployment to inflammatory sites. *Science* 2009; **325**: 612–616.
- 45 Looney MR, Thornton EE, Sen D, Lamm WJ, Glenn RW, Krummel MF. Stabilized imaging of immune surveillance in the mouse lung. *Nat Methods* 2011; **8**: 91–96.
- 46 Bajrmi B, Zhu H, Kwak HJ *et al.* G-CSF maintains controlled neutrophil mobilization during acute inflammation by negatively regulating CXCR2 signaling. *J Exp Med* 2016; **213**: 1999–2018.
- 47 Sitapara RA, Antoine DJ, Sharma L *et al.* The alpha7 nicotinic acetylcholine receptor agonist GTS-21 improves bacterial clearance in mice by restoring hyperoxia-compromised macrophage function. *Mol Med* 2014; **20**: 238–247.
- 48 Fernandez-Cabezudo MJ, Lorke DE, Azimullah S *et al.* Cholinergic stimulation of the immune system protects against lethal infection by *Salmonella enterica* serovar Typhimurium. *Immunology* 2010; **130**: 388–398.
- 49 Dhawan S, De Palma G, Willemze RA *et al.* Acetylcholine-producing T cells in the intestine regulate antimicrobial peptide expression and microbial diversity. *Am J Physiol Gastrointest Liver Physiol* 2016; **311**: G920–G933.
- 50 Dalli J, Colas RA, Arnardottir H, Serhan CN. Vagal regulation of group 3 innate lymphoid cells and the immunoresolvent PCTR1 controls infection resolution. *Immunity* 2017; **46**: 92–105.
- 51 Rankin LC, Girard-Madoux MJ, Seillet C *et al.* Complementarity and redundancy of IL-22-producing innate lymphoid cells. *Nat Immunol* 2016; **17**: 179–186.
- 52 Van Maele L, Carnoy C, Cayet D *et al.* Activation of Type 3 innate lymphoid cells and interleukin 22 secretion in the lungs during *Streptococcus pneumoniae* infection. *J Infect Dis* 2014; **210**: 493–503.
- 53 Liu GW, Bi YJ, Wang RN *et al.* Kinase AKT1 negatively controls neutrophil recruitment and function in mice. *J Immunol* 2013; **191**: 2680–2690.
- 54 Chen J, Tang HY, Hay N, Xu JS, Ye RD. Akt isoforms differentially regulate neutrophil functions. *Blood* 2010; **115**: 4237–4246.
- 55 Di Lorenzo A, Fernandez-Hernando C, Cirino G, Sessa WC. Akt1 is critical for acute inflammation and histamine-mediated vascular leakage. *Proc Natl Acad Sci USA* 2009; **106**: 14552–14557.
- 56 Gardai SJ, Hildeman DA, Frankel SK *et al.* Phosphorylation of Bax Ser184 by Akt regulates its activity and apoptosis in neutrophils. *J Biol Chem* 2004; **279**: 21085–21095.

- 57 Lee A, Whyte MK, Haslett C. Inhibition of apoptosis and prolongation of neutrophil functional longevity by inflammatory mediators. *J Leukoc Biol* 1993; **54**: 283–288.
- 58 Doua DN, Yip L, Khan MA, Grasemann H, Palaniyar N. Akt is essential to induce NADPH-dependent NETosis and to switch the neutrophil death to apoptosis. *Blood* 2014; **123**: 597–600.
- 59 Karimi K, Bienenstock J, Wang L, Forsythe P. The vagus nerve modulates CD4⁺ T cell activity. *Brain Behav Immun* 2010; **24**: 316–323.
- 60 Buijs RM, van der Vliet J, Garidou ML, Huitinga I, Escobar C. Spleen vagal denervation inhibits the production of antibodies to circulating antigens. *PLoS ONE* 2008; **3**: e3152.
- 61 Gautron L, Rutkowski JM, Burton MD, Wei W, Wan Y, Elmquist JK. Neuronal and nonneuronal cholinergic structures in the mouse gastrointestinal tract and spleen. *J Comp Neurol* 2013; **521**: 3741–3767.
- 62 Huston JM, Wang H, Ochani M *et al*. Splenectomy protects against sepsis lethality and reduces serum HMGB1 levels. *J Immunol* 2008; **181**: 3535–3539.
- 63 Teixeira FM, Fernandes BF, Rezende AB *et al*. *Staphylococcus aureus* infection after splenectomy and splenic autotransplantation in BALB/c mice. *Clin Exp Immunol* 2008; **154**: 255–263.
- 64 Chaudry IH, Tabata Y, Schleck S, Baue AE. Effect of splenectomy on reticuloendothelial function and survival following sepsis. *J Trauma* 1980; **20**: 649–656.
- 65 Grover GJ, Loegering DJ. Role of the liver in host defense to pneumococcus following splenectomy. *J Surg Res* 1984; **37**: 448–452.
- 66 Fernandes BF, Rezende AB, Alves CC *et al*. Splenic autotransplantation restores IL-17 production and antibody response to *Streptococcus pneumoniae* in splenectomized mice. *Transplant Immunol* 2010; **22**: 195–197.
- 67 van Westerloo D, van der Poll T. Acute vagotomy activates the cholinergic anti-inflammatory pathway. *Am J Physiol Heart Circul Physiol* 2005; **288**: H977–H978.
- 68 George MS, Sackeim HA, Rush AJ *et al*. Vagus nerve stimulation: a new tool for brain research and therapy. *Biol Psychiatry* 2000; **47**: 287–295.
- 69 Matute-Bello G, Frevert CW, Kajikawa O *et al*. Septic shock and acute lung injury in rabbits with peritonitis: failure of the neutrophil response to localized infection. *Am J Respir Crit Care Med* 2001; **163**: 234–243.

(Supplementary Information is linked to the online version of the paper on the *Cell Discovery* website.)



This work is licensed under a Creative Commons Attribution 4.0 International License. The images or other third party material in this article are included in the article's Creative Commons license, unless indicated otherwise in the credit line; if the material is not included under the Creative Commons license, users will need to obtain permission from the license holder to reproduce the material. To view a copy of this license, visit <http://creativecommons.org/licenses/by/4.0/>

© The Author(s) 2017